Science of the Total Environment 795 (2021) 148740

Contents lists available at ScienceDirect

Science of the Total Environment

journal homepage: www.elsevier.com/locate/scitotenv

The fate of Guadalquivir River discharges in the coastal strip of the Gulf of Cádiz. A study based on the linking of watershed catchment and hydrodynamic models

Juan J. Gomiz-Pascual [a,*], Marina Bolado-Penagos [a], Carlos J. Gonzalez [a], Agueda Vazquez [a], Cira Buonocore [a], Jeanette Romero-Cozar [a], Maria Luisa Perez-Cayeiro [b], Alfredo Izquierdo [a], Oscar Alvarez [a], Rafael Mañanes [a], Miguel Bruno [a]

[a] Department of Applied Physics, University of Cádiz, Cadiz 11510, Spain
[b] Department of Regional Geographic Analysis, University of Cádiz, Cadiz 11510, Spain

HIGHLIGHTS

- The hydrological model in the Guadalquivir basin has shown satisfactory results.
- The hydrodynamic model of Gulf of Cadiz and Strait of Gibraltar works well.
- Lagrangian model simulates the turbidity plume in concordance with satellite images.
- Rainfall coincides with winds from the western component.
- North, northwest or west winds: the plume develops towards the Strait of Gibraltar.

GRAPHICAL ABSTRACT

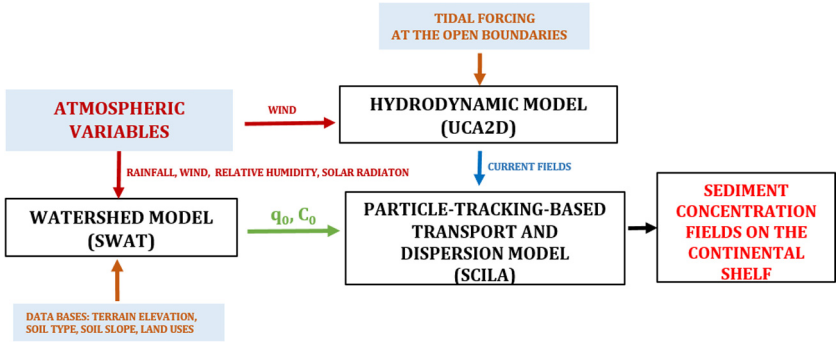

ARTICLE INFO

Article history:
Received 28 November 2020
Received in revised form 18 May 2021
Accepted 25 June 2021
Available online 3 July 2021

Editor: Víctor M. León

Keywords:
Hydrological and hydrodynamic models
Suspended solid transport
River discharges
Guadalquivir
Gulf of Cadiz
Strait of Gibraltar

ABSTRACT

A catchment model for river basins and a hydrodynamic model were combined in order to simulate the spreading of the turbidity plume produced by sediment discharges from the Guadalquivir River basin within the Gulf of Cádiz under different meteorological conditions. The current fields provided by the hydrodynamic model and a transport-diffusion scheme based on tracking virtual particles tracking released at the river mouth have enabled us to simulate turbidity plumes that show great similarity with the plumes observed in satellite images. The most relevant results of the study show that in the absence of winds, the plume tends to spread very slowly, gradually progressing northwards; this is because of the symmetry between the filling and draining flows at the mouth of the Guadalquivir and low intensity of the tidal currents beyond the mouth. In addition, the transport of the plume towards the Strait of Gibraltar requires wind conditions with a northerly, north-westerly or westerly component. Westwards transport, however, requires winds with an easterly, southerly, or south-easterly component. The periods of heaviest rainfall in the Guadalquivir River basin coincide with winds mainly from the west; therefore, the times of maximum discharge at the mouth of the river occur when there are wind conditions that favour the transport of the matter suspended in the plume, southwards along the coast, towards the Strait of Gibraltar and the Alboran Sea. Linking the watershed catchment and hydrodynamic models has proved its suitability to predict the evolution and reaching of the sediment plumes from the Guadalquivir River discharges and the experience encourages the use of that methodology to be applied in a future prediction system for the creation and evolution of those sediment plumes.

* Corresponding author.
E-mail address: juanjesus.gomiz@gm.uca.es (J.J. Gomiz-Pascual).

https://doi.org/10.1016/j.scitotenv.2021.148740

1. Introduction

The high complexity of systems formed by river basin-estuary-inshore coastal area makes the use of high performance computer models that simulate the physical evolution of land, atmospheric and oceanic processes an advantage for this study. Assuming the models are proven to reproduce realistic events (e.g. by means of hindcast validation), climatic and environmental processes can be studied effectively. However, such models will inevitably generate outputs that contain a level of uncertainty, due to assumptions of input variables and model parameterisations (Stainforth et al., 2005; Roe and Baker, 2007).

One of the most important current topics in this field of research is the development of a methodology to study how the contribution of organic matter from river estuaries to the open sea is predicted to change due to global warming. Many estuarine studies have drawn attention to the fact that the hydrological and thermal regimes of rivers are expected to change; these changes will directly affect freshwater ecosystems, water quality and human water use, as well as future volumes of primary production, and carbon cycling in epicontinental seas with low salinity (Khoroshevskaya, 2011; van Vliet et al., 2013). Estuaries also present high biochemical variability; for instance, there is a twice-daily influx of salt water intermixed with brackish or fresh water, and extreme physical and weather conditions, often producing strong tidal currents and turbidity. It is well-known that estuaries are subject to anthropogenic modifications, including dredging, land reclamation, deforestation, managed ecosystems, and coastal management, such as flood defences, construction of ports and harbours, industrialization, and discharges of polluted water, often containing solid industrial and domestic residues (e.g. plastic packaging and microparticles). The biochemical variability, together with diverse and severe anthropogenic modifications, make these systems extremely sensitive to climate change and difficult to study accurately and reliably. Nevertheless, a better understanding of estuarine processes, their responses to climate change, and the feedback to the environment, is fundamental for the sustainability of these ecosystems (Jones, 1994).

Although catchment, river, estuary, and sea comprise a unified dynamic system with profound interactions, they are often treated as separate entities in traditional modelling approaches. Each entity has been studied using different numerical models, operating at a range of spatial and temporal scales, and applied by scientists from different disciplines (e.g. hydrologists, civil engineers and oceanographers) (Warner et al., 2008a; Chen et al., 2013). Previously, the lack of computing capabilities was one of the obstacles hindering the study of the system as a whole. Information exchange between these entities (catchment, river, estuary and sea) is time consuming and promotes model-generated uncertainties. For example, it is worthless in terms of computational cost, to perform high-resolution simulations in one of the models, when the input data taken from another model do not offer the same level of resolution (Warner et al., 2008b).

The objective of the present study is inspired by the philosophy of the Land Ocean Interaction Study (LOIS) Project (Wilkinson et al., 1997) in that it emphasizes the link between hydrological events and their consequences in the coastal zone. This approach requires the use of hydrological models to determine how changes in land use, industrial inputs or climate influence the substances discharged by the rivers onto the continental shelves.

In the existing literature, the majority of the articles linking river and coastal dynamics are focused on the very nearshore side of the coastal zone and the issues assessed are located at the vicinity of the river mouths (Proctor et al., 2003; Uncles, 2003; Inoue et al., 2008; Meng et al., 2010).

However, there are only a few experiences where the Soil and Water Assessment Tool (hereinafter, SWAT) or similar catchment models have been used as input for a hydrodynamic model that simulates the behaviour of substances discharged by the rivers on the continental shelves over long distances (Bacopoulos et al., 2017). Moreover, there are several studies dealing with the linkage of river basin and lake hydrodynamics. In some of them, the catchment-process-based-model SWAT was used (Betrie et al., 2011; Zhang et al., 2017).

This study presents a feasibility assessment of the linking of the outputs of a catchment model, such as SWAT, with a hydrodynamic model that allows the diagnosis of the evolution of the concentration field of the discharged substances from the Guadalquivir river along the coastal strip of the Gulf of Cádiz.

The succeeding sections are organized as follows. In Section 2 the study region is presented. The data sources and methodology are described in Section 3. In Sections 4 and 5 the results are presented, describing the model performance and the results of the numerical experiments, followed by the discussion in Section 6; and finally, the main conclusions are presented in Section 7.

2. The study region

The Gulf of Cádiz (Fig. 1) is one of the most complex and interesting systems of the global ocean. It is an area of exchange and mixing between the Mediterranean Sea and the Atlantic Ocean, but it is also influenced by the northern arm of the Azores Current (Navarro and Ruiz, 2006). Superimposed on this general pattern, seasonality produces alternating regimes in surface waters together with an intense generation of mesoscale, which can modulate the exchange in the Strait of Gibraltar (Folkard et al., 1997). The coastal morphology strongly conditions the physical forcing, due to the existence of an abrupt change at Cape San Vicente (Fig. 1), where the western and southern coastlines converge, almost forming a right angle. Located to the east of the Cape is a large cove subjected to very intense water recirculation (Navarro and Ruiz, 2006). The general pattern of surface currents in the area is formed by an anticyclonic flow to the east above the continental slope extending to the Strait of Gibraltar, and counter-currents above the platform and in the open ocean (Folkard et al., 1997; Peliz and Fiuza, 1999; Relvas and Barton, 2002; Sanchez et al., 2006; Criado-Aldeanueva et al., 2006), forming cyclonic cells above the platform between the capes and an anticyclonic circulation in the central part of the Gulf. Both cells are connected by significant platform-continental slope-ocean exchanges (Sanchez and Relvas, 2003).

This pattern is commonly explained as a bimodal performance (west-southwest in winter and east from May to September) induced by wind forcing. However, recent studies show that the pattern is mainly determined, in one way or another, by the pressure gradient, not by local wind stress (Relvas and Barton, 2002); by the flow and buoyancy of continental inputs (Garcia-Lafuente et al., 2006); by convergence with the Azores Current (Sanchez and Relvas, 2003); by the exchange at the Strait of Gibraltar (Mauritzen et al., 2011; Peliz et al., 2009); or by the larger-scale wind regime (Sanchez et al., 2006).

In addition to the circulation pattern, the Gulf also receives a fresh water supply from the rivers Tinto and Odiel in the north, and more to the south, from two major rivers, the Guadiana and Guadalquivir (Gomez-Enri et al., 2012). The latter river is the most important contributor to the productivity of the Gulf, in comparison with the others (Huertas et al., 2005; Prieto et al., 2009).

The Guadalquivir River basin (Fig. 1) is a unique space located in southwestern Spain that possesses extraordinary natural, cultural, historical and economic value, where human activities have coexisted with the rich biodiversity of the river for many centuries: population settlements, traditional agriculture on the river banks and flood plain, leisure and recreation activities, fishing, paddy fields, among others (Ruiz et al., 2014). The estuary is navigable between the ocean and Seville (~110 km and 1.800 km^2 in area), and on its way to the mouth, it crosses the Doñana National Park, a UNESCO world heritage site and probably Spain's most important biosphere reserve (Ruiz et al., 2014).

The mean annual flow of the river at the Alcala del Rio monitoring station (Fig. 1) is 116.5 m^3/s (*Ministerio de Agricultura y Pesca, Alimentacion y Medio Ambiente;* Confederacion Hidrografica del

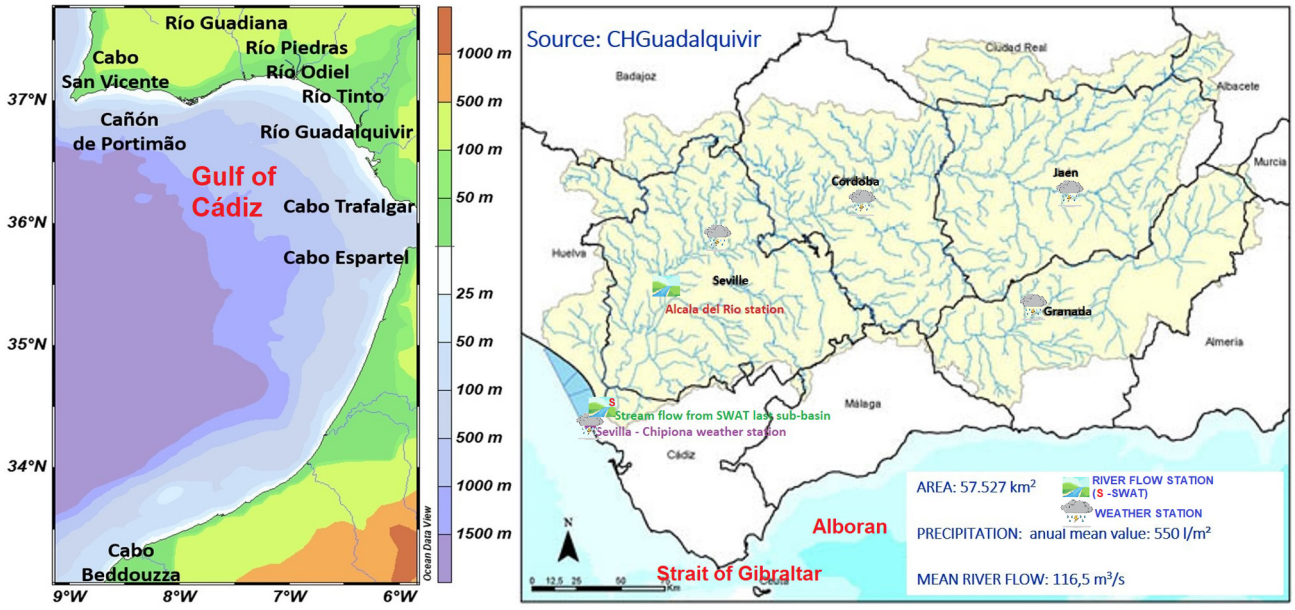

Fig. 1. Map of the study zone. Left: Gulf of Cádiz. Produced with Ocean Data View. Right: Hydrographic basin of the Guadalquivir, red: Alcala del Rio river flow station, purple: Sevilla-Chipiona weather station, green: the sub-basin output of SWAT where the river flow for the simulations was obtained and in black, over the basin, Seville, Cordoba, Jaen, and Granada where the weather stations were chosen. Source: www.chguadalquivir.es. (For interpretation of the references to colour in this figure legend, the reader is referred to the web version of this article.)

Guadalquivir (CHG), 2016 report). The river basin's annual precipitation averages 573 mm but with an irregular distribution due to the rainfall pattern of the area; for the wet months (November to April) the annual rate is 983 mm, and for the dry months (May to October) 260 mm. It must also be taken into account that half of an average year's total precipitation can occasionally be collected in just 24 h. These variations compound the effects of droughts or floods of the area (Borrego-Marin et al., 2015), and make the river susceptible to overflow, resulting in the inundation of much the adjacent land (Bath and Blomquist, 2004; Argüelles et al., 2012). Between 1st June and 30th September 2016, the hydrological resources measured at the Alcala del Rio station totalled 354 hm^3 for the whole four-month period (278 hm^3 at the Alcala del Rio dam and 76 hm^3 at the lower Guadalquivir canal); this water was used by the agriculture of the estuary, and to maintain the salinity balance of the paddy fields (CHG, 2016). This is an indicator of how important this sector is in the Guadalquivir basin and the importance of maintaining the water supply and water quality; the total water resources for the entire basin in the year 2015 comprised 3815.46 hm^3/year; of this total, 88% was used to meet the demands of agriculture, and 10% to meet urban demand. Aquaculture is another productive sector in the area that accounts for a large and increasing demand; recently, the total volume required was 142 hm^3/year (Berbel et al., 2015; CHG, 2016).

Therefore, this river basin with its large population (even considered to be overpopulated), substantial industry, agriculture, aquaculture, the natural park and other water users, is supporting considerable stress (Bath and Blomquist, 2004; Borrego et al., 2014), and is under continuous study and management to maintain the correct balance between natural flow, water demand, and water quality. The main land uses in the basin are forestry (49.1%), agriculture (47.2%), urban areas (1.9%) and wetlands (1.8%) (CHG, 2016). All these factors must be incorporated into the hydrological model, which is the main reason why SWAT was used in this study (Gomiz-Pascual et al., 2016). This analytical tool can be easily modified to take into account changes in land uses, water supplies and soil; thus the output variables of river flow volume, sediment transport, content in phosphates, nitrates, nitrites, among other, can quickly be recalculated (Narsimlu et al., 2013).

Several studies have reported the relationship among turbidity plumes, nutrients and phytoplankton response in the Guadalquivir estuary and adjacent coastal areas. Mendiguchia et al. (2007) show how turbidity plumes can be characterized biogeochemically by their significant content of inorganic nutrients. Moreover, Navarro and Ruiz (2006), analysing satellite images of sea surface chlorophyll concentration acquired by a SeaWIFS sensor, identified the development of a chlorophyll plume associated to the Guadalquivir river discharges. Finally, Caballero et al. (2014), based on the analysis of Ocean Colour MODIS (Moderate Resolution Imaging Spectrometer) satellite images, found a clear relationship between the Guadalquivir turbidity plumes and the appearance of phytoplankton blooms along the coastal strip of the Gulf of Cádiz. The same authors found that the phytoplankton response along the coastal strip is delayed with respect to the peaks of sediment load from the river, which is explained by the light limitation on the phytoplankton growth produced by the sediment-induced turbidity.

Turbidity patterns in this area have also been well explained using satellite sensors (Caballero and Navarro, 2016). In the work reported here, the occurrences of heavy rainfalls are related to increased flow rates from the Alcala del Rio dam, and both processes with the plume of turbidity. Moreover, the rainfall occurrence seems to show a close correlation with the NAO (North Atlantic Oscillation), showing that part of its interannual variability is associated with this index, with the river flow being the mechanism regulating the turbidity pattern in periods of heavy rainfall (Navarro et al., 2011); whereas the hydrodynamics of the area (a sediment plume associated with the tidal cycle is always present) determine the plume during the rest of the year (Caballero et al., 2011). Within the Gulf of Cádiz, it is observed that, due to the area's own hydrodynamics, the plume usually travels close to the coastline towards the south-east; and the largest plumes that have been observed are associated with riverine discharges due to storm flood events (Prieto et al., 2009; Caballero et al., 2014), and have extended from the mouth of the estuary southwards almost as far as the Strait of Gibraltar, and close to the coast (Fig. 1) (Caballero et al., 2014).

3. Data sources and methodology

For this study different data (river flow, rainfall, temperature, wind, tidal harmonic constants and satellite data) have been used. Table 1 shows information about the used data sources. In the map in Fig. 1

Table 1
Information about time resolution and source for the data used in the study.

Data	Resolution	Source
River flow	Daily mean	Spanish Ministry of Agriculture and Fisheries, Food and Environment (MAPAMA) http://sig.mapama.es/redes-seguimiento/
Meteorological data	Daily mean	Agro Climatic stations from Andalusian Regional Government http://www.juntadeandalucia.es/agriculturaypesca/ifapa/ria/servlet/FrontController
Digital Elevation Model (DEM)	1 arc-second (~30 m)	Shuttle Radar Topography Mission (SRTM) European Space Agency
Land use	100 m	Coordination of Information on the Environment (CORINE) version 1.3
Soil type	5 arc-second (~150 m)	FAO (Food and Agriculture Organization) version 3.6
True-color images	3-Bands combination band 1-RED(620–670 nm) band 4-GREEN(545–565 nm) band 3-BLUE(459–479 nm) 1 km	True-Color RGB MODIS-Aqua https://aeronet.gsfc.nasa.gov/new_web/data_usage.html
Chlorophyll images	L2 wave length nLw555 1 km	MODIS Aqua sensor - http://oceancolor.gsfc.nasa.gov/
Tides	M2 and S2 amplitude and phase from different points	Different sources. See Section 5.2., Table 4.

the study area in shown with indication of the data precedence and other locations of interest.

The analysis methodology was based on three basic elements:

(i) The catchment model (SWAT) where the hydrology has been satisfactorily resolved taking into account the clime, dams, soil types, and land uses.
(ii) The hydrodynamic model (UCA2D) forced with the M2 and S2 tidal constituents (main tidal constituents of the study area) and wind, for surface water mass circulation simulation along the coastal strip of the Gulf of Cádiz.
(iii) A transport and dispersion model, based on particle tracking, of the sediment plumes produced by the Guadalquivir River discharges. This model is fed by daily mean, flow and sediment concentration supplied by the SWAT model and current velocity fields supplied by the UCA2D model.

The sketch in Fig. 2 illustrates the way in which the three different models are linked to each other. More details about the way the models and the data are used in the analysis will be left for the following sections, before describing the corresponding results.

4. Analysis of the observations

4.1. Rain and wind regimes at the adjacent coastal area

Studies, such as Borrego-Marin et al. (2015), Bath and Blomquist (2004), and Argüelles et al. (2012), demonstrate a relationship between the rainfall and the river flow despite the high regulation of the river by dams. This relationship is even more clear in the estuary due to the influence of the last dam before the mouth, which is not as important. In addition, this relationship between rainfall, flow volume and plume can be corroborated by the studies published by Navarro et al. (2011) and Caballero et al. (2011). These studies revealed the relationship that exists between the intensity of the turbidity plume and periods of heavy rain, with a large plume being formed just after an event of heavy rainfall. The plume is fairly well-differentiated and much larger than the small plume of sediments associated with the tidal transport.

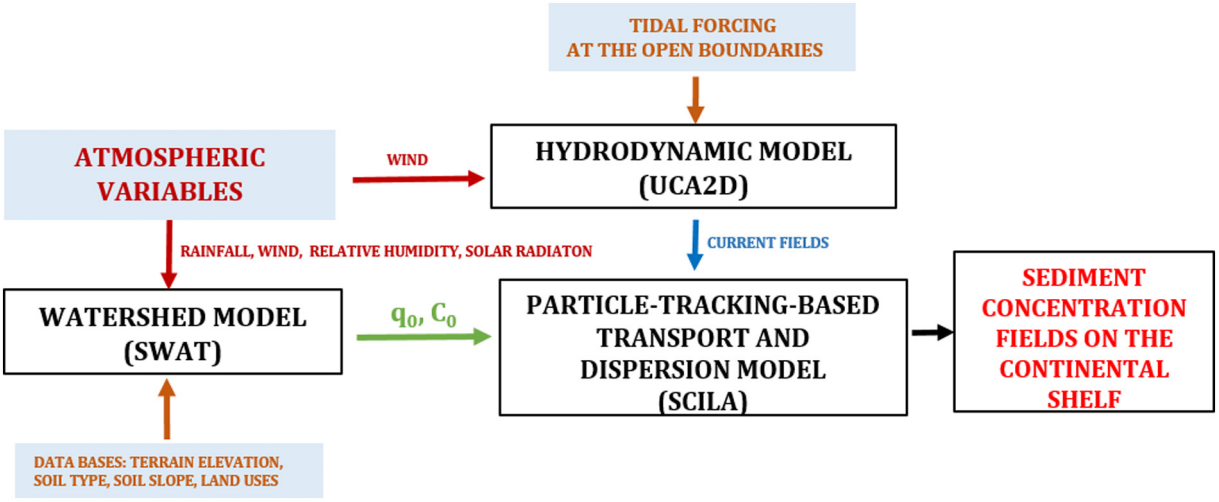

Fig. 2. Explicative diagram showing the interconnection between the different tools involved in the prediction of sediment concentration produced by the rainfall occurrence on the watershed. Inside the white filled rectangles and with black text the three main tools of the predictive system are indicated: The hydrodnamic model (UCA2D), the watershed tool (SWAT), and the transport and dispersion model (SCILA). The sediment concentration field is the output (as indicated by the black arrow) of the predictive system (emphasized with red text) from the transport and dispersion model. The other arrows indicate the input data (specified the shaded rectangles) required from each tool and which output variables from the hydrodynamic and watershed model are transferred to the transport and dispersion model. The different sources for the needed input data are described in Section 3. (For interpretation of the references to colour in this figure legend, the reader is referred to the web version of this article.)

Wind data provided by *Puertos del Estado* from the Sevilla-Chipiona Weather Station (Fig. 1), were analysed for the period between 2012 and 2016; a wind rose was drawn for each year, together with a wind rose for the complete period (Fig. 3). Table 2 presents the % occurrence, maximum, minimum (≠ 0) and average values for the eight principal wind directions (N, NE, NW, E, W, S, SW, and

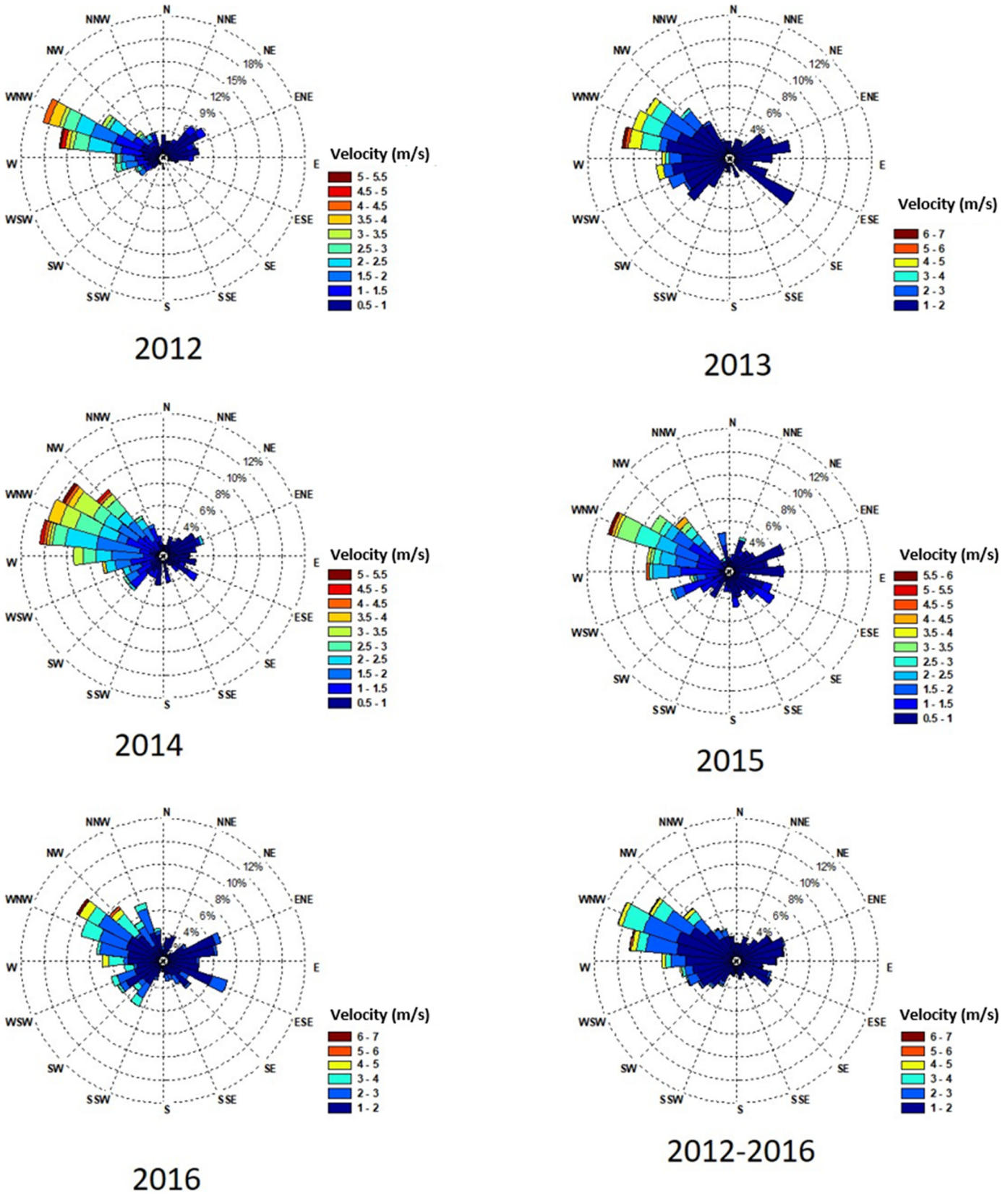

Fig. 3. Wind roses by years, and similarly, wind rose with the complete period of study. Data from Sevilla-Chipiona Weather Station. (For interpretation of the references to colour in this figure legend, the reader is referred to the web version of this article.)

Table 2
Table of winds recorded in the zone during the period between 2012 and 2016.

Direction	(247.00°-292.50°)		(292.50°-337.50°)		(22.50°-67.50°)		(67.50°-112.50°)	
% Occurrence	30.89		28.78		17.96		7.35	
	mod (m/s)	dir (°)	mod (m/s)	dir (°)	mod (m/s)	dir (°)	mod (m/s)	dir (°)
Max	9.30	272.10	8.00	305.60	8.40	62.50	8.40	92.10
Min	0.10	255.10	0.10	303.70	0.10	57.40	0.20	82.50
Avg.	2.26	260.49	2.30	305.21	1.39	53.58	1.13	86.50
Direction	(112.50°-157.50°)		(337.50°-22.50°)		(202.50°-247.50°)		(157.50°-202.5.50°)	
% Occurrence	6.38		3.60		3.17		1.87	
	mod (m/s)	dir (°)	mod (m/s)	dir (°)	mod (m/s)	dir (°)	mod (m/s)	dir (°)
Max	7.60	112.80	4.10	4.30	5.00	218.70	4.10	188.70
Min	0.20	137.60	0.20	353.60	0.20	209.10	0.20	191.10
Avg.	1.40	127.29	1.27	0.34	1.35	213.48	1.17	180.10

SE). As mentioned in the introduction, it was observed that both westerly and easterly winds are the two most characteristic of the zone, with the greatest intensities recorded in the periods of westerly wind.

4.2. Satellite images vs river flow

Figs. 4 and 5 show images of turbidity and concentration of Chl-*a*. By analysing them the possible relationship of these variables with the

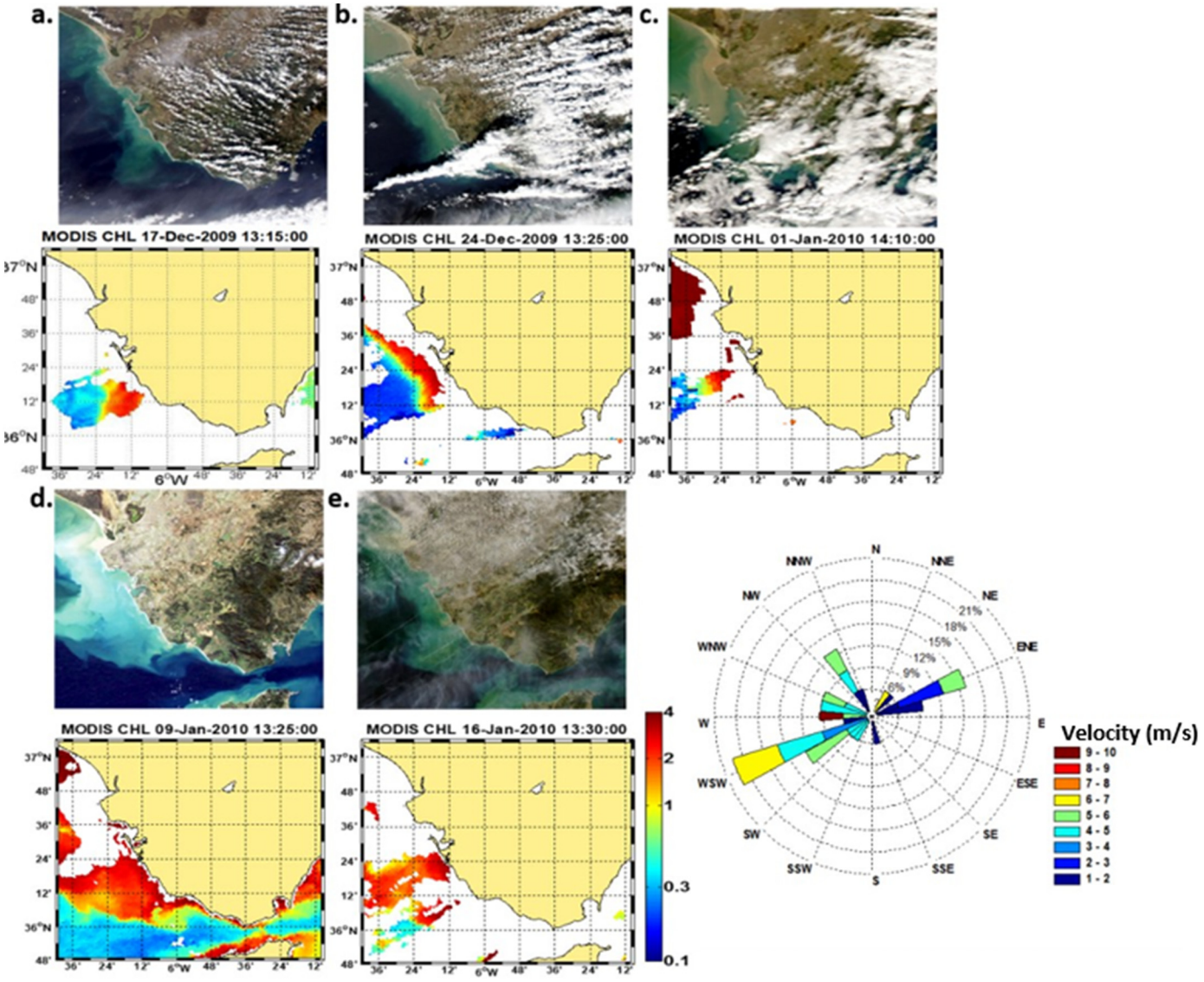

Fig. 4. MODIS Aqua images of True Colour and Ocean Colour (Chl-*a*)) MODIS (a. 17th December, b. 24th December 2009, c. 1st January, d. 9th January and e. 16th January 2010) and a wind rose for the period of study corresponding to a season of heavy rainfall (from 17th December 2009 to 16th January 2010) Data from Sevilla-Chipiona Weather Station. (For interpretation of the references to colour in this figure legend, the reader is referred to the web version of this article.)

intensity of the river's discharges can be studied. A connection between low/high discharges and less/greater presence of the turbidity plume can be seen at the mouth of the estuary.

Fig. 4 corresponds to a period of intense precipitation that occurred between the end of 2009 and the beginning of 2010, and with predominance of westerly winds. The period of rain started on 18th December 2009 after a period of at least two weeks without significant rain. Fig. 4a shows the turbidity right before the rain event started and Fig. 4b corresponds to the situation six days later. Fig. 4c is an image taken just a week after the start of the rain and after four days of persistent rain. Lastly, Fig. 4d corresponds to five days after an event of substantial rain that occurred on 4th January 2010. Satellite imagery enables us to infer the evolution of the turbidity plume over the course of one month from the start of the rains. These reached their greatest intensity on 4th January 2010, and then gradually diminished in intensity until stopping completely.

On the other side, Fig. 5 shows the evolution of the turbidity plume over the course of a month, during a period of drought that occurred in the summer of 2007 and predominance of westerly winds. The satellite images correspond to the month of July 2007 during a period of drought. However, during this period certain rainfall events associated with summer storms were recorded; these began on 12th July and lasted, with a few breaks, until 22th July. The effects of these rains on the turbidity plume are made evident in Fig. 5d, which corresponds to nine days after the start of the storms; this figure shows a somewhat more developed plume than in the rest of the images. That plume, however, does not develop the intensity of those shown for the period of rains to shown in Fig. 4. Fig. 5e that corresponds to 29th July 2007, a week after the rains stopped, shows merely a trace of the turbidity plume.

5. Models performance

5.1. SWAT model

The catchment model SWAT was chosen to simulate the hydrology of the estuary, based on the good performance in previous studies carried out by the authors (Gomiz-Pascual et al., 2016). In addition, it is a Fortran-based open source model, actively supported by the United States Department of Agriculture. SWAT is a river basin scale model that has been in use for the past three decades, developed to quantify the impact of land management practices in large, complex watersheds. It simulates the quality and quantity of surface and ground water and predicts the environmental impact of land use, land management practices, and climate change. SWAT is a long time scale simulation model. It requires input information about weather and climate, soil properties,

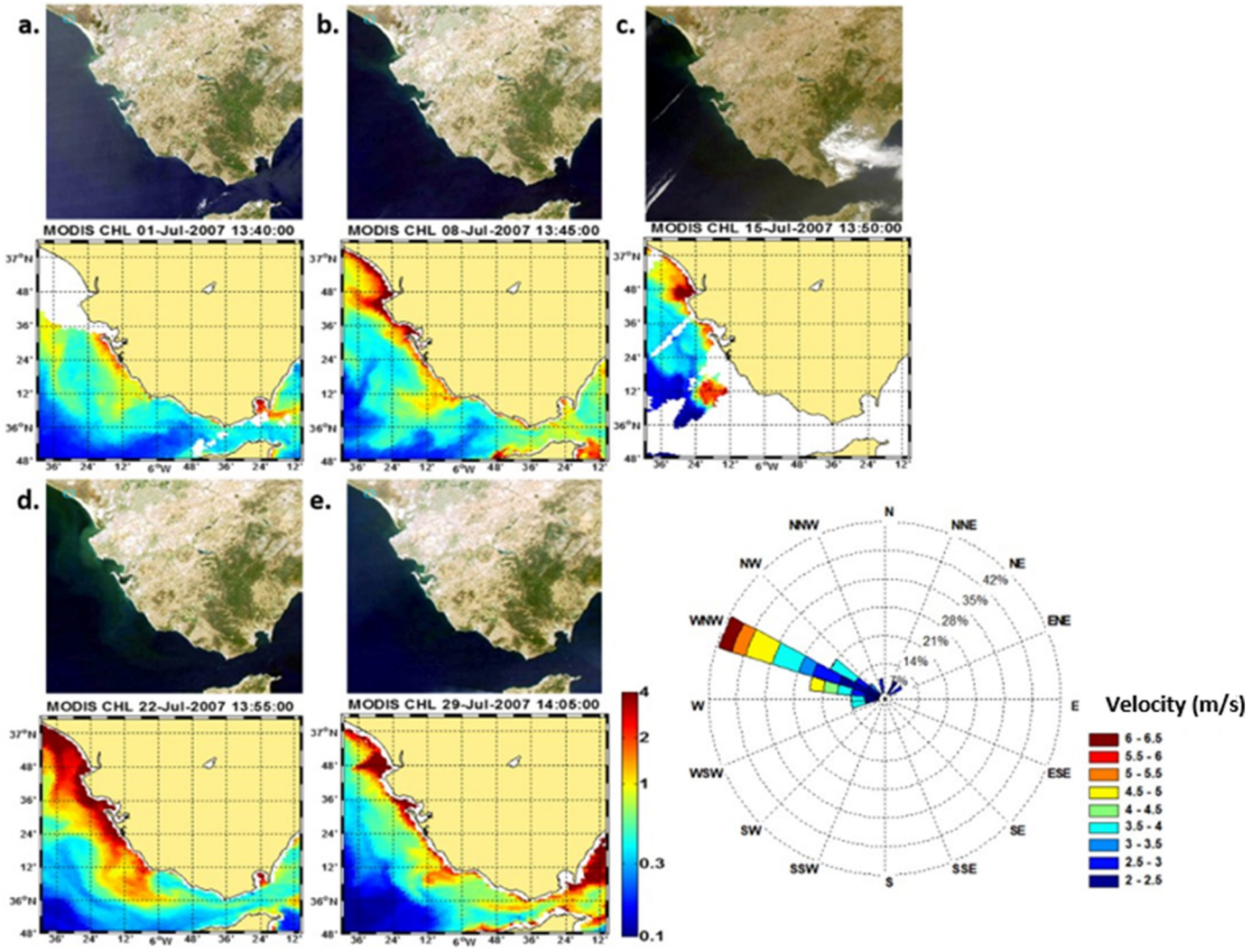

Fig. 5. MODIS Aqua images of True Colour and Ocean Colour (Chl-*a*)) MODIS (a. 1st July, b. 8th July, c. 15th July, d. 22nd July and e. 29th July of 2007) and a wind rose for the period of study corresponding to a season of low rainfall Data (from 1st July 2007 to 29th July 2007) Data from Sevilla-Chipiona Weather Station. (For interpretation of the references to colour in this figure legend, the reader is referred to the web version of this article.)

topography, vegetation, and land uses. The physical processes associated with the water, sediments, and nutrients are calculated and interconnected by the different modules used by SWAT and described in studies, such as Neitsch et al. (2011) and Arnold et al. (1990, 1995). Considering that the Guadalquivir estuary is a highly complex system, subject to continuous changes, all these factors must be taken into account when developing a hydrological model. In this regard, SWAT is an adaptive model that allows changes in soil types, land uses, and the shape of the river as well as recalculation of the output variables (i.e. sediment or nutrient concentration) in an easy way.

For the computation of daily flows, the formula given by Simić et al. (2009) is used, while for the calculation of total sediment transport (bottom load + suspended load) the Soulsby-Van Rijn formula (Soulsby, 1997) is used. For the calculation of potential evapotranspiration, the programme allows the user to choose among three possible methods: Hargreaves, Priestley-Taylor, and Penman-Monteith. The Hargreaves method only requires temperature and solar radiation data to calculate evapotranspiration (Hargreaves and Sumani, 1985; Hargreaves and Allen, 2003). The Penman-Monteith method is considered the most adequate and was used in the present study. In terms of input data, this method requires the following: daily solar radiation, maximum temperature, minimum temperature, maximum relative humidity, minimum relative humidity, and wind speed (Allen et al., 2006; Walter et al., 2005).

For the validation of SWAT observations of daily discharged we chose flows that are available from the hydrological station of Alcala del Rio (see Fig. 1). Due to the scarcity of daily time series of sediment concentration observations in the river, these were not included in the validation procedure.

The validation based on river flow observations was performed following the methodology described in Gomiz-Pascual et al. (2016), in which the SWAT hydrological model was calibrated and validated for the Guadalquivir basins . The first step was to perform a new validation for two extreme conditions represented by a month of intense rain (December 2009–January 2010), and drought conditions (July 2007), respectively. Atmospheric data that comprise rainfall, air temperature,

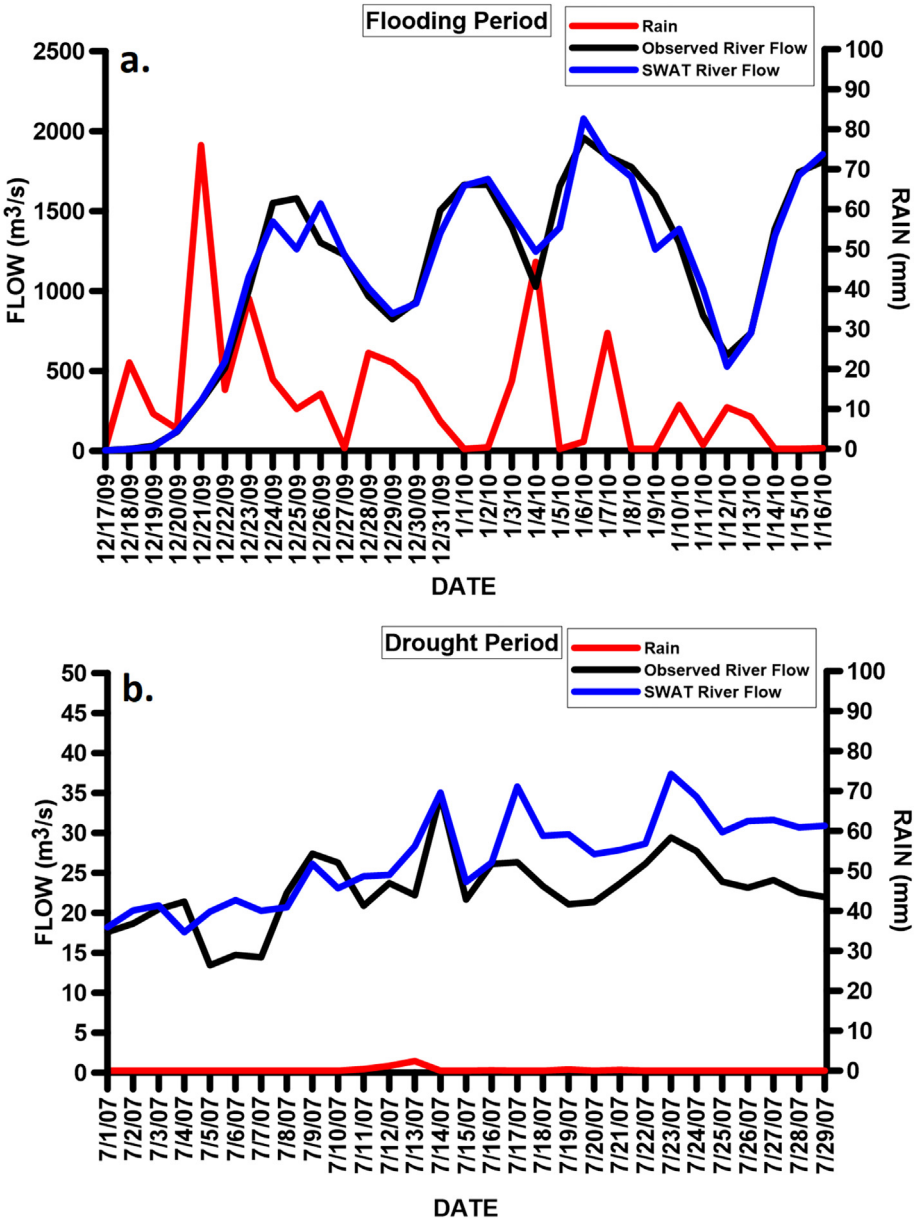

Fig. 6. Flow volume of the river at the Alcala del Rio Station vs result of the flow rate modelled by SWAT in the sub-basin where the Alcala del Rio Station is located. a. between 17th December 2009 and 16th January 2010, corresponding to the period of heavy rain; b. between 1st and 29th July 2007 when there was a period of drought during which there was a serious storm resulting in rapid flooding on July 21st. Rainfall data from Seville meteorological station.

solar radiation, and relative humidity were provided by four stations located at Jaen, Cordoba, Granada and Seville (see Fig. 1 and Table 1), covering the whole watershed from 2005 to 2014. Moreover, additional information about terrain elevation, land-uses, soil types, and land slope were needed. DEM, the land-use map, and the soil-type map were in ESRI format to be used in ArcGIS, while the database with all the different parameters needed for the different layers of the different soils to be run in SWAT was calculated following the SWAT user manual.

River flow data were recorded at the Alcala del Rio Station for a period of one month of intense rain (December–January 2009–2010), and for a period of drought (July 2007). They were used to compare the modelled and observed flow rates. Both periods were chosen in order to meet two basic criteria: firstly, and most importantly, these were periods in which flooding was caused by heavy rain and serious droughts were recorded; the second criterion was that the period offered the least possible cloud cover in order to have a better visualization of the sediment plume created by the river discharges using satellite images. These discharged flows simulated with SWAT were compared with data recorded in Alcala del Rio. As can be seen in Fig. 6, and as expected from the results of Gomiz-Pascual et al. (2016), the maximum flow rates are slightly overestimated, whereas the minimum flow rates are slightly underestimated. In general, SWAT reproduces the discharged flow in this part of the river fairly accurately, with respect the observed values.

Although not used to validate SWAT sediment outputs because of the scarcity of daily observed data, we were able to include the sediment concentration for extreme and mean flow situations using the available sediment observations from 1/1/2005 to 12/31/2014 after being interpolated to fill time gaps using the United States Geological Survey (USGS) FORTRAN programme LOAD ESTimator (LOADEST) (Cakir et al., 2019; Buonocore et al., 2021) and after comparing LOADEST values and SWAT outputs. LOADEST provides an estimate of the sediment load as a function of observed daily river flow. That function is determined by performing a linear regression analysis between the available sediment concentration observations and the corresponding river flow data. This way, sediment concentration may be interpolated for the same days of river flow data and compared with SWAT output values. Table 3 shows good agreement between observed river flow and modelled river data (SWAT) and sediments between LOADEST (interpolated observation data) and SWAT.

The obtained values for the corresponding river flows (average, maximum and minimum) are shown in Table 3.

5.2. UCA2D hydrodynamic model

The UCA2D hydrodynamic model was chosen for this study, showing a satisfactory performance in reproducing several hydrodynamic processes in the Gulf of Cádiz (Alvarez et al., 1999, 2003; Gonzalez et al., 2018) and also with wind forcing (Gonzalez et al., 2018, 2019). This model solves the vertically-averaged equations of mass conservation and momentum (that is, the currents calculated represent the mean value for the whole water column, which is very representative in a shallow environment, such as that under study). The numerical model resolves the system of equations by means of a Crank-Nicolson semi-implicit method in finite differences on an Arakawa type-C grid, which confers great stability and accuracy to the numerical solution. Each time step (from n to n + 1) is subdivided into two "half passages"; in the first one, $u^{n+1/2}$ and $\xi^{n+1/2}$ are implicitly resolved while $v^{n+1/2}$ is explicitly calculated, while in the second half-step v^{n+1} and ξ^{n+1} they are implicitly resolved and u^{n+1} explicitly. Here, u, v and ξ are the zonal and meridional components of current velocity and sea surface elevation, respectively. The discrete system of equations is completed with the imposition of solid boundary conditions (coast line: free-slip and impenetrability) and open boundary conditions (forcing) in liquid contours (connection with open sea: amplitudes and phases of elevation and speed for the tidal components considered, assumed a sinusoidal variation over time).

In the open boundary, the so-called "radiative velocity condition" can also be imposed (Reid and Bodine, 1968; Flather and Heaps, 1975), so that the numerical disturbances generated within the model domain are radiated out.

In each simulation, the elevation fields ξ (x, y, t) and velocities u (x, y, t), v (x, y, t) are obtained at regular intervals of time Δt. Additionally, the model spatially integrates the equations of momentum and continuity in order to quantify the energy associated with each term thereof, and obtain a total energy balance at each moment, which should tend towards null values to ensure the conservative nature of the system, as well as the stability of the numerical solution. The model also takes into account the stresses by friction with the bottom and by effect of the wind on the surface, by means of the parameterization known as logarithmic law ("law of the wall"). The outputs of the model in terms of the present needs are the elevation of the water surface with respect to the local average sea level and the velocity of the current (vertically averaged) at each grid node of the grid for the instants of time desired.

The UCA2D model was executed using a grid with a resolution of 1 × 1 km, with a time step of five seconds, and simulated three cycles of neap and spring tides, in such a way that the first 15 days were used as spin-up period, and the following two tidal cycles (30 days) were subsequently used as results of the simulations. The simulation was carried out taking into account the M2 and S2 tidal components. The mesh covers the area shown in Fig. 7. In order to validate the model, amplitudes and phases of both components were compared with harmonic constants obtained from the measurement stations and provided by different sources (see Table 4), whereas the tidal currents were compared only with data from the Cádiz Station. In our case, it can be seen that the UCA2D model resolved the elevations fairly well, with errors in the amplitude for the M2 constituent of 4.2%, and for the S2 of 7.7%, errors in the M2 phase of 8.1 min, for S2 of 9.6 min, and in the tidal currents as can be seen in Table 4. Taking into account that in the model we assume a fixed depth of 10 m, when within the Bay of Cádiz, the mean depth is approximately 8 m, and at some points only 4 m, which means that the reduction of velocity by friction with the bottom is more than that calculated by the model, it can be concluded that the model reproduces the observed currents reasonably well.

The maps of amplitude and phases for the principal semi diurnal waves are shown in Fig. 7, where the Gulf of Cádiz presents a clear wave diffraction pattern matching the different tidal regimes of the Strait of Gibraltar and the North Atlantic, and in accordance with other simulations done in the same area (Izquierdo and Mikolajewicz, 2019; Candela et al., 2019).

5.3. Simulation of the transport and dispersion of the river plume in different wind and rain conditions

In this study, the transport/dispersion of Guadalquivir River discharges to the Gulf of Cádiz were simulated using a Lagrangian particle-tracking model, with proven suitability in many similar

Table 3
Representative values of river flow and suspended solids concentration in periods of low, average, and heavy rainfall. The analysis period spans from 01/01/2005 to 31/12/2014, a total of 3652 days of observations. Among these days, 138 days correspond to drought periods, 147 days to heavy rain periods, and 3367 to normal days.

Flow rates m^3/s			
TOTAL DAYS: 3652 (10 YEARS)	Drought 138/3652	Normal 3367/3652	Rains 147/3652
Maximum	34.77	440.89	1958.93
Minimum	13.44	3.51	119.99
Average	22.79	116.50	1125.97
Suspended solids mg/L			
Maximum	128.00	1884.00	3656.00
Minimum	32.00	10.90	118.00
Average	86.75	361.60	577.00

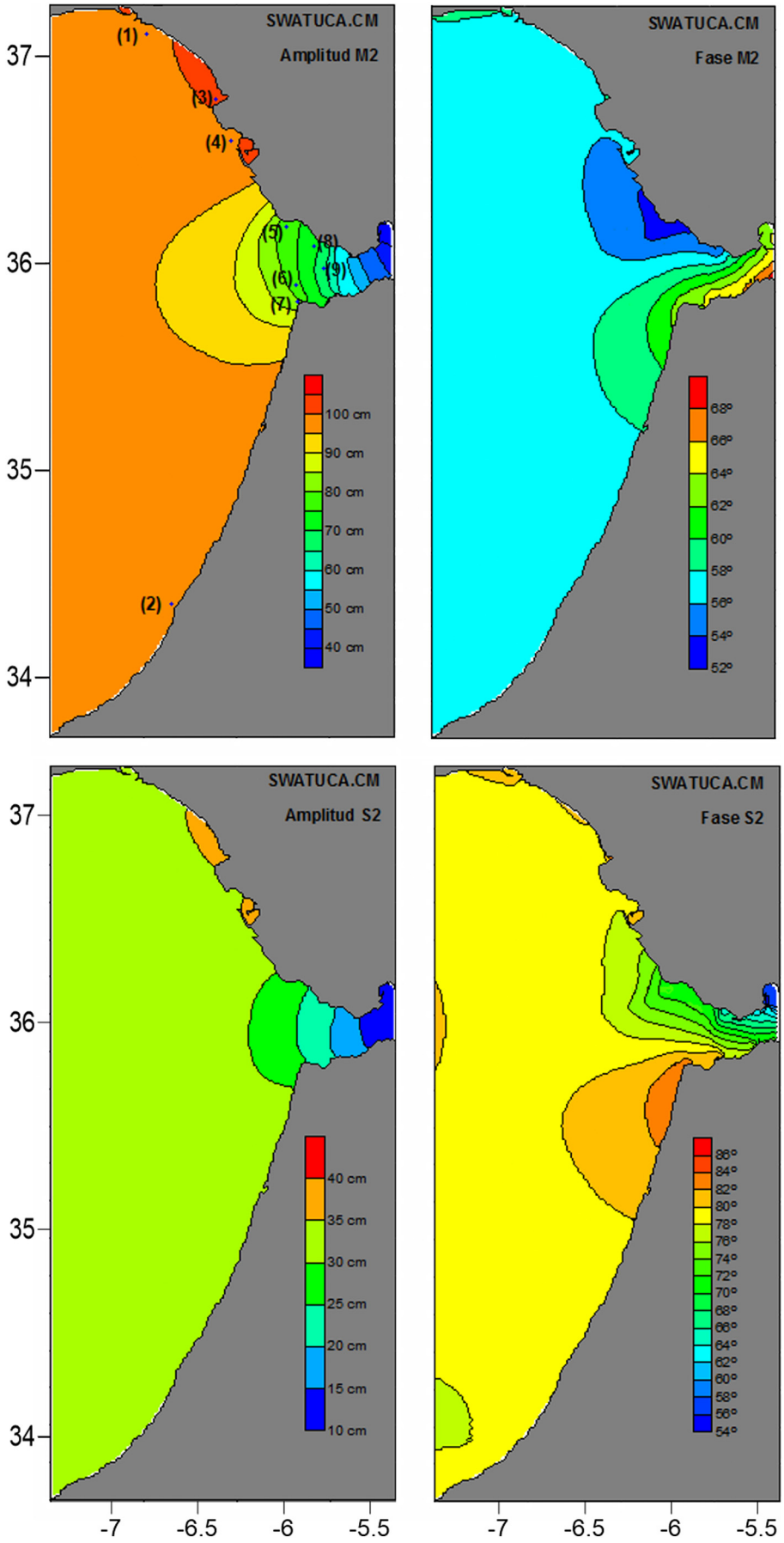

Fig. 7. Amplitude and phase for the constituents of M2 and S2 tides calculated with the UCA2D.

Table 4
Validation of the hydrodynamic simulations: tides.

M2 elevation

Station	Lon (°E)	Lat (°N)	Amplitude (cm)		Phase (°Green.)	
			Observed	Modelled	Observed	Calculated
Mazagón (1)	−6.83	37.13	105.9	99.2	57.2	57.5
Medina (2)	−6.70	34.36	95.3	96.7	56.0	56.6
Cadiz (3)	−6.34	36.60	102.9	99.0	54.1	55.9
Chipiona (4)	−6.42	36.75	103.7	101.6	54.7	56.8
C. Trafalgar (5)	−6.03	36.17	76.2	77.2	53.5	53.0
DW (6)	−5.97	35.88	78.5	77.0	56.1	60.2
Espartel (5)	−5.94	35.78	75.8	80.9	67.0	62.4
Pta. Gracia (5)	−5.81	36.08	64.9	71.3	49.0	55.2
DN (6)	−5.77	35.97	60.1	66.5	51.8	58.8
RMSE			4.4 cm (4.2%)		3.9° (8.1 min.)	

S2 Elevation

Station	Lon (°E)	Lat (°N)	Amplitude (cm)		Phase (°Green.)	
			Observed	Modelled	Observed	Calculated
Mazagón (1)	−6.83	37.13	38.6	34.5	83.9	79.9
Cadiz (3)	−6.34	36.60	35.1	34.5	82.3	78.5
Chipiona (4)	−6.42	36.75	37.1	35.4	76.8	79.6
C. Trafalgar (5)	−6.03	36.17	27.9	26.3	77.0	70.6
DW (6)	−5.97	35.88	29.0	25.1	82.2	78.9
Espartel (5)	−5.94	35.78	25.7	26.3	92.0	82.6
Pta. Gracia (5)	−5.81	36.08	22.3	23.6	74.0	71.5
DN (6)	−5.77	35.97	22.5	21.2	73.8	73.8
RMSE			2.3 cm (7.7%)		4.8° (9.6 min.)	

Tidal currents. Cadiz Station (3)

Const.	Major semiaxis (cm/s)		Minor semiaxis (cm/s)		Phase (°Green.)		Inclination (°)	
	Obs.	Mod.	Obs.	Mod.	Obs.	Mod.	Obs.	Mod.
M2	6.7	16.8	−0.5	−2.4	335.5	330.0	8.2	22.6
S2	2.9	7.2	−0.1	−0.7	1.3	3.3	4.1	13.3

Sources: (1) Puertos del Estado; (2) Le Provost et al. (1995). (3) Alvarez et al., 1999. (4) Alvarez et al., 2003. (5) Garcia Lafuente (1986). (6) Candela (1990).

applications (Gonzalez et al., 2018, 2019). In this model the particle tracking is assumed to be determined by the advective and dispersive transport related to the 2-D horizontal, depth averaged current velocity field. The position of each "spillet" particle (in this context, it may be thought as a 'parcel' of discharged water) at any time is given by:

$$\mathbf{p}_{i+1} = \mathbf{p}_i + \mathbf{u}_i \Delta t + \boldsymbol{\delta} \quad (1)$$

where $\mathbf{p}_i$ are $\mathbf{u}_i$ are, respectively, the horizontal vectors of a particle's position and current velocity, calculated by the model UCA2D forced by tide and winds, at the i-th multiple of the time-step Δt. The vector term $\boldsymbol{\delta}$ accounts for the turbulent diffusion, computed according to a 2-D random-walk model (Csanady, 1973) as $\boldsymbol{\delta} = \mathbf{r}\, 2D_H \Delta t$, where D_H is the horizontal turbulent diffusion coefficient, assumed to be time-constant and spatially-homogeneous, and $\mathbf{r} = rx\,\mathbf{i} + ry\,\mathbf{j}$ is a horizontal two dimensional vector whose components take random values, according to a normal distribution with mean 0 and standard deviation 1 (Matsuzaki and Fujita, 2014), and $\mathbf{i}$, $\mathbf{j}$ are unit vectors. D_H was set at 2.0 m^2/s, estimated from the current velocity fluctuations measured in the study area by González et al. (2010).

The mass amount of substance discharged from the river through a time lapse Δt, may be written as $\Delta m_i = C_0\, q_0\, \Delta t$, where q_0 is the flow rate (m^3/s). Alternatively the mass amount may be expressed in terms of the number of particles released at the mouth at each Δt, n_i, by:

$$\Delta m_0 = \alpha\, n_0 = C_0 q_0 \Delta t \quad (2)$$

In order to optimize the computational time, we determined the minimum number of particles to be released at the river mouth at each time step Δt, allowing an adequate description of the discharge plume. After a sensitivity analysis a releasing rate of 10 particles was chosen, each $\Delta t = 30$ min. This analysis showed differences of less than 10% with respect to a rate of 100 particles every 30 min (Fig. 8). Taking the values of discharged flows (q_0) representative of the mean and heavy rainfall periods and their corresponding sediment concentration (C_0) shown in Table 2, we determined the values of the constant α for each period using Eq. (2).

Subsequently, the substance concentration found in every node of the domain at each time step Δt may be computed as:

$$C(x,y,t) = \frac{\alpha\, n(x,y,t)}{aH} \quad (3)$$

being $n(x,y,t)$ the number of particles found within a given node of size $\Delta x \Delta y$ at each time instant; a is the horizontal area of the node; H is the mean bottom depth in the area.

Fig. 2 synthesizes the linking between the different procedures involved in the simulation of the transport and dispersion of the sediment plumes produced by the river, in response to the heavy rainfall episodes on the watershed. On the one hand, rainfall data and other atmospheric variables, in combination with other features of the watershed, are used by SWAT to compute the flow rate (q_0) and sediment concentration (C_0) at the mouth of the river. On the other hand, the hydrodynamic model forced by wind and tides supplies the current velocity fields that, along with the values q_0 and C_0 provided by SWAT, feed the particle-tracking-based transport and dispersion model.

Following the calibration and validation of the different numerical models, a series of numerical experiments was designed to analyse the processes of transport and dispersion of the plume along the coastal strip of the Gulf of Cádiz using the numerical procedure described in the previous section and illustrated in Fig. 2. The main aim was to assess the performance of the proposed set of predictive tools, focusing firstly on

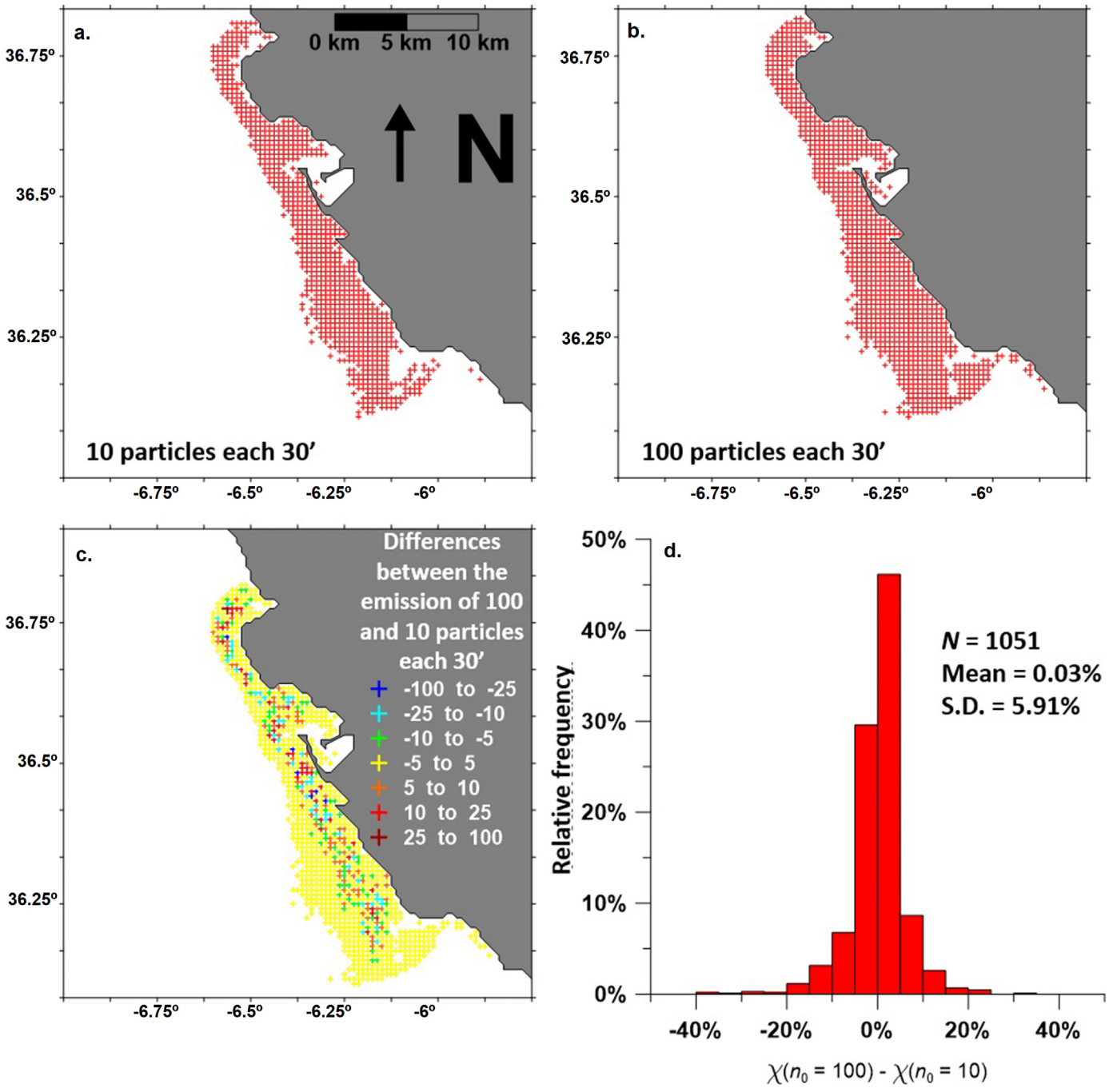

Fig. 8. a. Graph showing the simulation at one month with 10 particles every 30′; b. Graph showing the simulation at one month with 100 particles every 30′; c. Differences between the emission of 100 and 10 particles each 30′; d. This graph is the histogram of frequencies for the differences between the (Chi) χ values obtained in two simulations identical in all respects (wind from the W, high rainfall flow volume) except in the rate of emission of particles: 100 particles/time step, and 10 particles/step time, respectively.

the response to three characteristic situations: average, heavy, and minimal rainfall. The characteristic values for river flow and sediment concentration corresponding to these situations are extracted from the performance of a 10-year simulation of daily values. Among these simulations the three characteristic values matching the three aforementioned rainfall situations were chosen. These values are shown in Table 3 with their corresponding observed ones. The good agreement between the simulated and observed values provides additional confidence and reliability to the performed SWAT predictions.

Following this idea, a total of 18 simulations were executed taking as input the sediment concentration corresponding to the average and heavy rain situations shown in Table 3. For each rainfall situation eight wind directions were considered (northeast, north, northwest, east, west, southwest, south and southeast), with a wind intensity of 10 m/s, and a situation of no wind, or calm.

The results obtained in these experiments are presented in Figs. 9 and 10, where the colour of the particles indicates the number of days since their releasing. With respect to the experiments of average flow rate (Fig. 9), it can be observed that, in the absence of wind (e.), the particulate matter remains trapped close to the river mouth; however, with northerly winds (b.), westerly winds (d.), or from the north with a westerly (a.) or easterly component (c.), the turbidity plume spreads southwards, staying close to the coast, towards the Strait. With winds from the southeast (i), southwest (g.), south (h.) or east (f.), the plume spreads northward, again staying close to the coastline, towards the coast of Portugal.

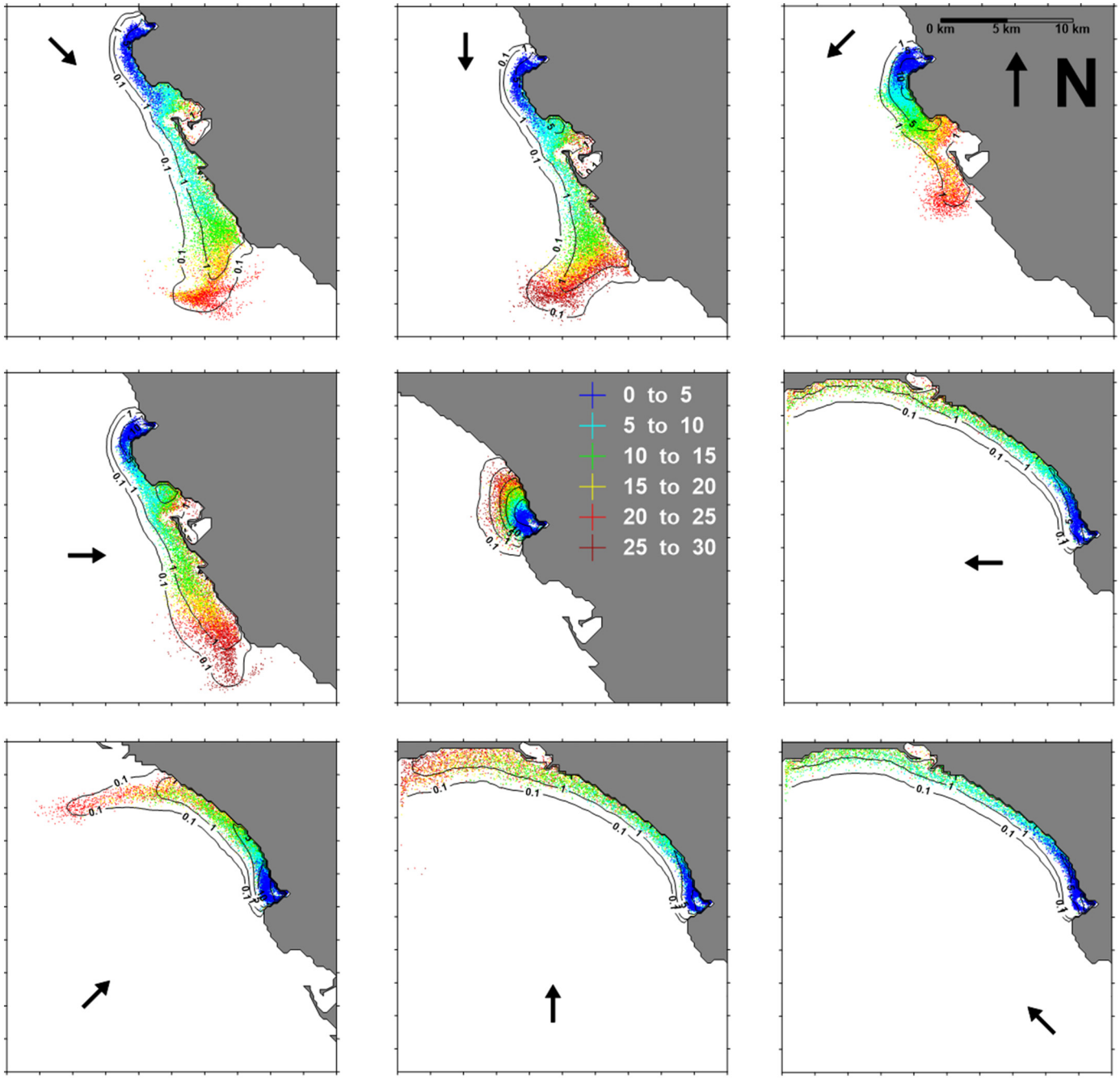

Fig. 9. Lagrangian experiment for average flow rate of the Guadalquivir, from blue (more recent particles) to red (older particles). Concentration fields of suspended sediments (mg/L) originating from the river Guadalquivir. Black arrows indicate wind direction. (For interpretation of the references to colour in this figure legend, the reader is referred to the web version of this article.)

The evolution of the plume towards the Strait is faster when the wind is from the north (b.) or northwest (a.), taking approximately seven days to reach the western end of the Strait. With wind from the west (d.), the plume needs at least 14 days to reach the western end of the Strait. The evolution of the plume towards the Portuguese coast, however, is more rapid with winds from the east (f.) or southeast (i.), and takes around seven days to reach the coast of the Algarve.

With flow rates typical of heavy rains (Fig. 10), practically the same behaviour can be observed, although the plume is further developed and presents a greater content of particulate matter at the western side of the Strait. The accumulation of particles in this zone also takes place in the experiment with average discharge flow, albeit less pronounced.

It is important to note that, for the cases when the plume spreads towards the Strait, with both average and high flow rate, a tendency was observed for the particulate matter to accumulate close to Cape Trafalgar.

6. Discussion

In the preceding sections, it can be seen that the utilization of the SWAT tool in the watershed of the Guadalquivir River gives fairly reasonable results, particularly with respect to the estimation of the flow rates in response to the rainfall occurrences in the basin. Therefore, SWAT seems to be an adequate tool for specifying the flow rates that produce the plume of turbidity that subsequently spreads along the

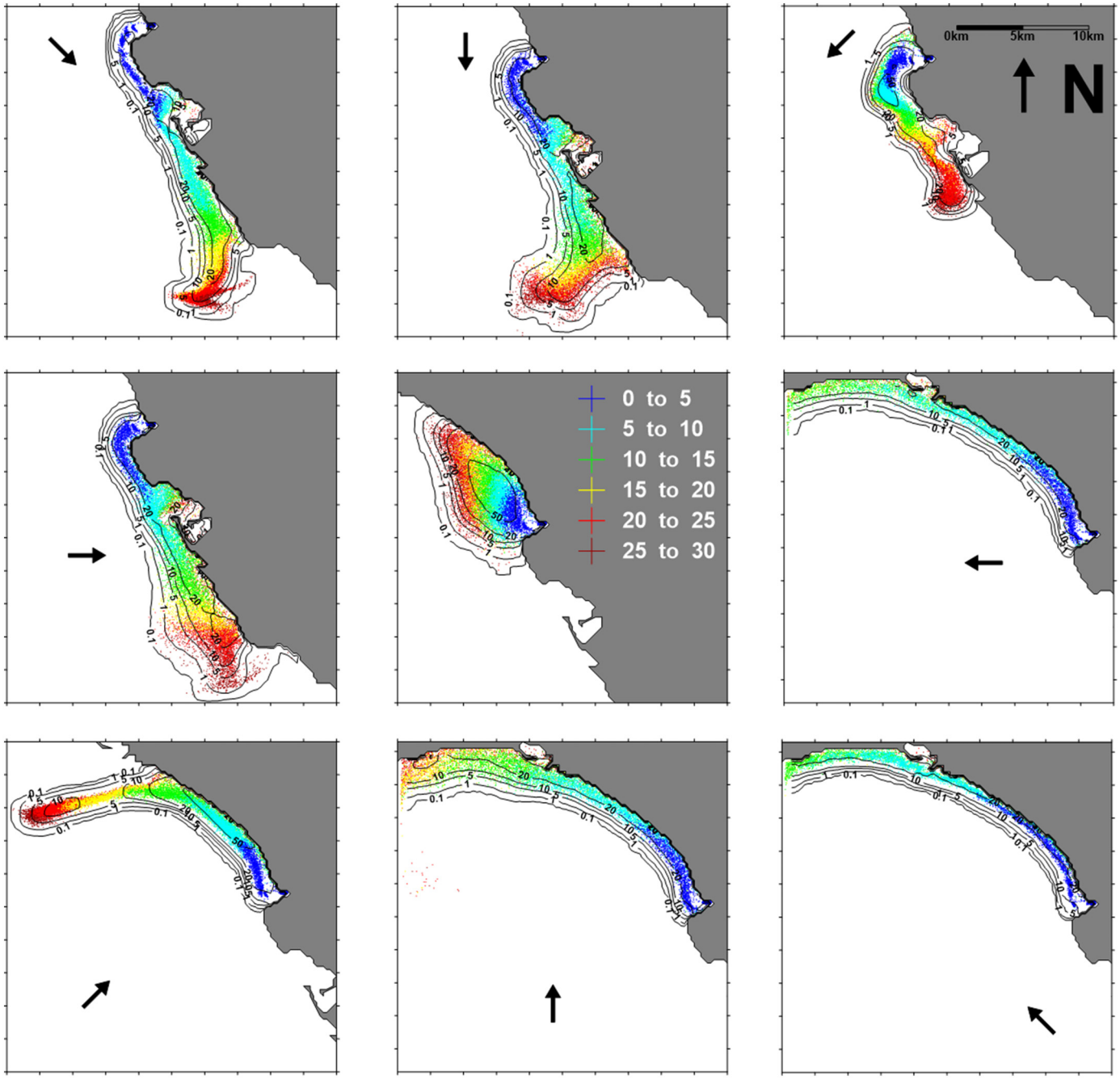

Fig. 10. Lagrangian experiment for heavy-rainfall flow rate of the Guadalquivir, from blue (more recent particles) to red (older particles). Concentration fields of suspended sediments (mg/L) originating from the river Guadalquivir. Black arrows indicate wind direction. (For interpretation of the references to colour in this figure legend, the reader is referred to the web version of this article.)

coastal strip of the Gulf. Moreover, this process of transport and dispersion of the sediment plume seems to be correctly described with the particle-tracking approach proposed in Gonzalez et al., 2018, 2019) and fed by the current fields simulated by the UCA2D barotropic model.

The good behaviour of the used numerical procedure as a tool for forecasting the evolution of the turbidity plume, becomes evident when we compare the image of turbidity of Fig. 4 with the distribution of the plume simulated using the UCA2D model, shown in Figs. 9 and 10 (for northerly, northwesterly and easterly wind directions). The image in Fig. 4b was obtained six days after a rainfall event had begun following a period of at least two weeks without significant rains. Considering that the plume was not present before the rainfall event that began on 18th December 2009, it can be estimated from this image that the plume took approximately six days to reach the western end of the Strait. This time taken for the plume to travel corresponds fairly well to the time obtained from the numerical experiments using the hydrodynamic model, that is, about seven days. It has to be added that the actual wind conditions in the period between 18th and 24th December 2009 were quite similar to those used in the simulations carried out.

There is also a good agreement between these simulations and the image of turbidity in Fig. 5d corresponding to a summer period with lower values of precipitation and river discharge. In this case, also considering that the plume was non-existent before the start of the first rainfall event on 13th July 2007, the time taken for the plume to travel from the mouth to the western end of the Strait, estimated on the basis of the image, is about nine days.

In the absence of wind, the plume tends to disperse very slowly, progressing very gradually towards the north; this is due to the symmetry of the filling and emptying flows at the mouth of the Guadalquivir, and to the weakness of the current just beyond the mouth. The diversion northwards is a genuine effect of the Coriolis force. The movement of the plume towards the Strait of Gibraltar requires that the ruling weather conditions correspond to winds from the north, northwest, or west. In contrast, the movement of the plume towards the west requires winds from the east, south, or southeast.

Regarding the sediment concentration fields in the strip adjacent to the coast line, the concentration for the situation of heavy rainfall (maximum flow rate) is 10 times greater than the concentration corresponding to the situation of average rainfall (average flow rate). Of special consideration is the accumulation of sediments specifically in the zone of Cape Trafalgar where other authors found a clear accumulation of phytoplankton and high retention capacity (e.g. Sala et al., 2018; Bolado-Penagos et al., 2020). Also, once it has reached that zone, the spreading of the plume tip evolves into a sort of filament that extends towards the open sea. This characteristic can also be identified when comparing Fig. 9 (for winds from the north, northwest, and east) with Figs. 4 and 5.

The explanation for the accumulation of sediment (and other substances, such as phytoplankton) near Cape Trafalgar may be provided by the current fields simulated by the UCA2D model. The maps of average current obtained for three types of forcing are shown in Fig. 11: left, tides only (not wind); centre, tides and easterly wind; and right, tides and westerly wind. In the map of average velocity corresponding to the experiment with tidal forcing only, this average circulation tends to take the shape of a vortex in the shallower waters off Cape Trafalgar. This illustrates the principal mechanism by which the particulate matter stays trapped in this zone. The accumulation of particles produced by this structure of the field of average current is strongly changed under the wind forcing. With a westerly wind, the field of average current varies notably with respect to that obtained in the simulation without wind. The average current is intensified in the direction towards the Strait along the coastal strip, to the west of Trafalgar. However, a zone of almost zero average current continues to be produced just to the east of Trafalgar, creating a front between the waters to the north and south of Cape Trafalgar.

In the simulation forced with easterly wind the average current is intensified towards the Portuguese coast, along the whole coastal strip of the Gulf. This average current towards Portugal prevents the transport of the turbidity plume towards the Strait; the plume takes the form reproduced by the Lagrangian model (Fig. 10).

Another interesting aspect is the possible relationship between the occurrence of precipitation and the occurrence of winds from a direction of origin that would facilitate the transport of the plume towards the Strait of Gibraltar. In this regard, the joint distribution of precipitations and winds in the study zone were analysed, with the help of a graph that may conveniently be called a rainfall rose. This rose is analogous to the wind rose, but instead of illustrating the strength and direction of the winds during a set period of time, the daily rainfall and the daily average direction of the wind are represented. This rainfall rose, produced for the 2005–2014 period, is presented in Fig. 12. It can be seen that a significant proportion of the rainfall in the Guadalquivir basin was recorded coinciding with the occurrence of westerly winds. This coincidence of westerly winds and rainfall is of special importance, since it implies that at the times of greatest discharge from the river, the plume tends to move towards the Strait. This development implies the transport of the matter suspended in the plume, and the other substances and properties associated with that body of water, along the coastal strip towards the Strait of Gibraltar and the Alboran Sea. among The most relevant among the transported substances are nutrients and phytoplankton, which interact with each other. On the one hand, the nutrients that are discharged with the plume contribute towards the growth of phytoplankton along the coastal strip of the Gulf of Cádiz (Navarro and Ruiz, 2006; Mendiguchia et al., 2007; Caballero et al., 2011), which consumes part of the nutrients present. On the other hand, both the phytoplankton and remaining nutrients are transported towards the Strait and, through the Strait, as far as the Alboran Sea, along the coastline. Once these substances reach the coastal edge of the Strait, it is expected that the processes of water upwelling at the interface, or nearby, continue supplying nutrients to these inshore waters (Bruno et al., 2013; Bolado-Penagos et al., 2020); this would enable the transported phytoplankton to continue growing while passing through the Strait, and when it reaches the Alboran Sea, thus contributing significantly to the growth of the phytoplankton in this latter region.

Linking the watershed catchment and hydrodynamic models has proved its ability to predict the evolution and reaching of the sediment plumes from the Guadalquivir river discharges and the experience encourage the use of the used methodology to be applied in a future

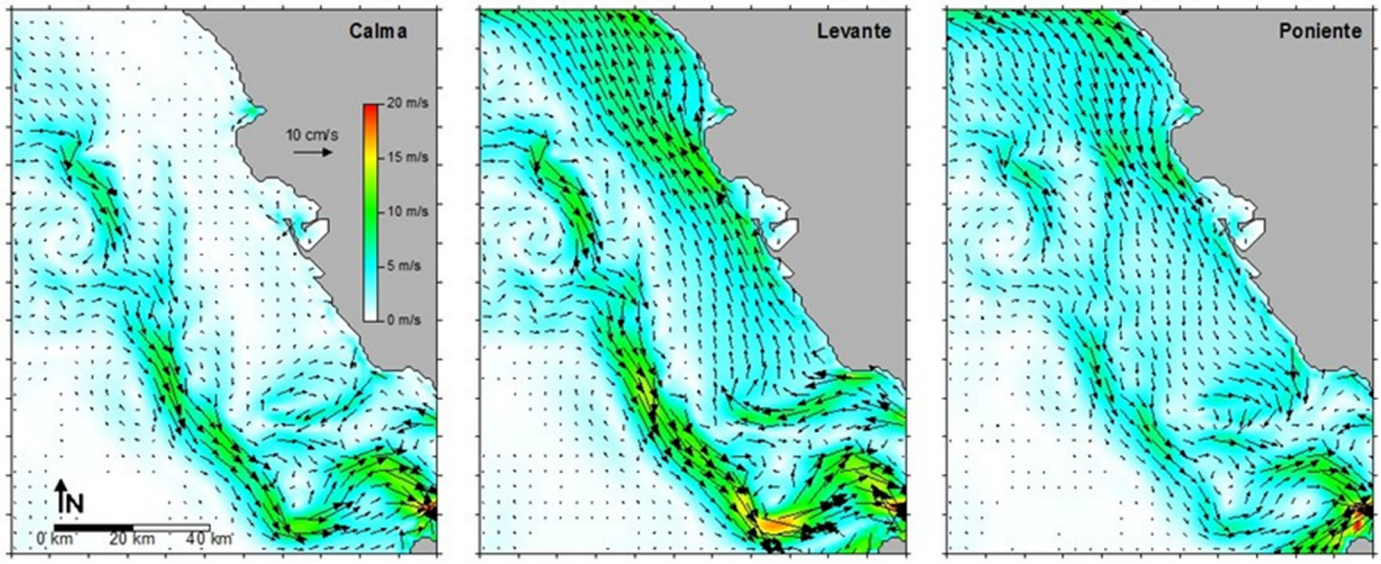

Fig. 11. Average velocity fields of the current corresponding to the output of the hydrodynamics simulation experiments carried out with the UCA2D model. Left: tidal forcing only; Centre: with tides and easterly wind; Right: with westerly wind.

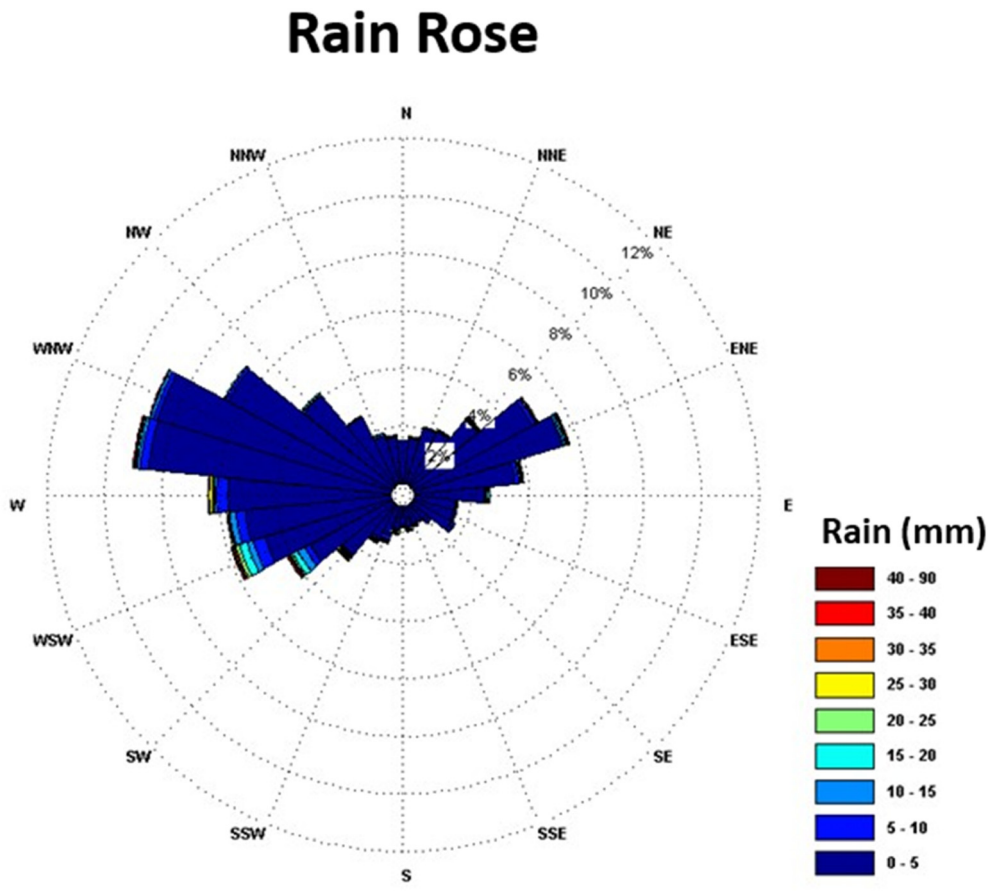

Fig. 12. Rainfall rose for the period between 1st January 2005 and 31st December 2014 in the study area. Data from Sevilla-Chipiona weather station. (For interpretation of the references to colour in this figure legend, the reader is referred to the web version of this article.)

prediction system for the creation and evolution of the sediment plumes that appear to trigger an important biological response, in terms of phytoplankton growth, along the Gulf of Cádiz coast and even as far as the western part of the Alboran Sea.

7. Conclusions

The implementation, calibration, and subsequent validation of the SWAT tool in the Guadalquivir River basin have shown satisfactory results, supporting its use in the evaluation of the river flow discharges, starting with the rainfall in the basin as input data. The UCA2D hydrodynamic model, forced with tide and wind, satisfactorily reproduces the hydrodynamics of the Gulf of Cádiz coastal strip. The Lagrangian model fed with the velocity fields of the current provided by the hydrodynamic model, allows simulations of the turbidity plume that show close similarity with the plumes observed in satellite images. In the absence of winds, the plume tends to spread very slowly progressing gradually northwards; this is due to the symmetry of the filling and draining flows at the mouth of the Guadalquivir and the low intensity of the current beyond the mouth. The diversion to the north is a genuine effect of the Coriolis force. The movement of the plume towards the Strait of Gibraltar requires prevalence of wind conditions with a northern, northwestern or western component. Movement westwards, however, requires winds with an eastern, southern or southeastern component. The periods of the heaviest rainfall in the Guadalquivir basin coincide with winds with a western component. Therefore, the times of maximum discharge at the mouth of the river occur under conditions that favour the transport along the coastal strip of the particulate matter suspended in the plume and the diverse substances conveyed by these waters, with their particular properties, towards the Strait of Gibraltar and the Alboran Sea. Linking the watershed catchment and hydrodynamic models has proved its suitability in predicting the evolution and reaching of the sediment plumes from the Guadalquivir River discharges. Therefore, the proposed methodology may form the basis of a future prediction system to simulate the creation and evolution of events of important biological impacts in the studied area.

CRediT authorship contribution statement

JJGP performed the data analysis and processing under supervision from MB and AV. JJGP wrote the manuscript with the help and inputs from all co-authors. All authors contributed to the article and approved the submitted version.

Declaration of competing interest

The authors declare that they have no known competing financial interests or personal relationships that could have appeared to influence the work reported in this paper.

Acknowledgements

We would like to thank the Regional Government of Andalusia (P11-RNM-7722 project), the Spanish Government (TRUCO project RTI2018-100865-B-C22), the SUDOE INTERREG AGUAMOD and OCASO projects for supporting this work financially. We are also grateful to NASA for distributing the MODIS data used in this study, and to the AERONET project for the MODIS AQUA RGB True Color Images, especially those from the Malaga-San Jose and Huelva stations.

References

Allen, R.G., Pereira, L.S., Raes, D. y, Smith, M., 2006. Evapotranspiracion del cultivo, Organizacion de las Naciones Unidas para la Agricultura y la Alimentacion (FAO). vol. 56 pp. 1–79.

Alvarez, O., Izquierdo, A., Tejedor, B., Mañanes, R., Tejedor, L., Kagan, B.A., 1999. The influence of sediment load on tidal dynamics, a case study: Cadiz Bay. Estuar. Coast. Shelf Sci. 48, 439–450. https://doi.org/10.1006/ecss.1998.0432.

Alvarez, O., Tejedor, B., Tejedor, L., Kagan, B.A., 2003. A note on sea-breeze-induced seasonal variability in the K1 tidal constants in Cadiz Bay, Spain. Estuar. Coast. Shelf Sci. 58 (4), 805–812.

Argüelles, A., Berbel, J., Gutierrez-Martin, C., 2012. La evolucion de la Cuenca del Guadalquivir (España). Rev. Obras Públicas 159 (3537), 51–64.

Arnold, J.G., Williams, J.R., Nicks, A.D., Sammons, N.B., 1990. SWRRB: A Basin Scale Simulation Model for Soil and Water Resources Management. Texas AandM Univ. Press, College Station, TX, p. 1990.

Arnold, J.G., Williams, J.R., Maidment, D.R., 1995. Continuous-time water and sediment-routing model for large basins. J. Hydraul. Eng. 121 (2), 171–183, 1995.

Bacopoulos, P., Tang, Y., Wang, D., Hagen, S.C., 2017. Integrated hydrologic-hydrodynamic modeling of estuarine-riverine flooding: 2008 tropical storm fay. J. Hydrol. Eng. 22 (8), 1–11.

Bath, A., Blomquist, W., 2004. Policy, politics, and water management in the Guadalquivir River Basin, Spain. Water Resour. Res. 40 (8-7).

Berbel, J., Gutierrez, C., Borrego-Martin, M.M., 2015. System of Water Accounting in Guadalquivir River Basin (SYWAG) Final Report. Publisher: Universidad de Cordoba.

Betrie, G.D., van Griensven, A., Mohamed, Y.A., Popescu, I., Mynett, A.E., Hummel, S., 2011. Linking SWAT and SOBEK using Open Modeling Interface (OpenMI) for sediment transport simulation in the Blue Nile River Basin. Trans. ASABE 54 (5), 1749–1757.

Bolado-Penagos, M., Gonzalez, C.J., Chioua, J., Sala, I., Gomiz-Pascual, J.J., Vazquez, A., Bruno, M., 2020. Submesoscale processes in the coastal margins of the Strait of Gibraltar. The Trafalgar – Alboran connection. Prog. Oceanogr. 181, 102219.

Borrego, M.M., Perales, J.M., Berbel, J., 2014. Metodologia para elaboracion de cuentas hibridas SEEA-W. Proyecto SYWAG (System of Water Accounting in Guadalquivir River Basin). Working Paper Departamento de Economia Agraria, Universidad de Cordoba http://hdl.handle.net/10396/12360.

Borrego-Marin, M.M., Perales, J.M., Gutierrez-Martin, C., Berbel, J., 2015. Analysis of Guadalquivir Droughts 2004-2012 Based on SEEA-W Tables, International Conference on DROUGHT. Research and Science-Policy Interfacing, Valencia.

Bruno, M., Chioua, J., Romero, J., Vazquez, A., Macias, D., Dastis, C., Ramirez-Romero, E., Echevarria, F., Reyes, J., Garcia, C.M., 2013. The importance of sub-mesoscale processes for the exchange of properties through the Strait of Gibraltar. Progress in Oceanography. vol. 116.

Buonocore, C., Gomiz-Pascual, J.J., Pérez-Cayeiro, M.L., Mañanes-Salinas, R., Bruno-Mejías, M., 2021. Modelling the impacts of climate and land use changes on water quality in the Guadiana basin and the adjacent coastal area. STOTEN 776, 146034.

Caballero, I., Navarro, G., 2016. Analisis multisensor para el estudio de los patrones de turbidez en el estuario del Guadalquivir. Rev. Teledeteccion 46, 1–17. https://doi.org/10.4995/raet.2016.5717.

Caballero, I., Ruiz, J., Navarro, G., 2011. Dynamics of the turbidity plume in the Guadalquivir estuary (SW Spain): a remote sensing approach. OCEANS https://doi.org/10.1109/Oceans-Spain.2011.6003489.

Caballero, I., Morris, E.P., Prieto, L., Navarro, G., 2014. The influence of the Guadalquivir River on the spatio-temporal variability of suspended solids and chlorophyll in the Eastern Gulf of Cadiz. Mediterr. Mar. Sci. 721–738.

Cakir, R., Raimonet, M., Sauvage, S., Paredes-Arquiola, J., Grusson, Y., Roset, L., Meaurio, M., Navarro, E., Sevilla-Callejo, M., Lechuga-Crespo, J.L., Gomiz Pascual, J.J., Bodoque, J.M., Sanchez-Perez, J.M., 2019. Hydrological alteration index as an indicator of the calibration complexity of water quantity and quality modeling in the context of global change. Water 12, 15. https://doi.org/10.3390/w12010115.

Candela, J., 1990. The barotropic tide in the Strait of Gibraltar. In: Pratt, L.J. (Ed.), The Physical Oceanography of Sea Straits. Kluwer, Dordrecht, pp. 457–475.

Candela, J., Izquierdo, A., Mikolajewicz, U., 2019. The M2 tide diffraction at the Strait of Gibraltar. Rapp. Comm. int. Mer Medit. 42, 24.

Chen, W.B., Liu, W.C., Wu, C.Y., 2013. Coupling of a one-dimensional river routing model and a three-dimensional ocean model to predict overbank flows in a complex river–ocean system. Appl. Math. Model. 37 (9), 6163–6176.

Confederacion Hidrografica del Guadalquivir Plan Hidrologico de la demarcacion hidrografica del Guadalquivir, 2016. Real Decreto 1/2016. http://www.chguadalquivir.es/descargas/PlanHidrologico2015-2021/Planes_2DO_Ciclo/Guadalquivir/MEMORIA_PHD_GUADALQUIVIR.pdf (173 pp.).

Criado-Aldeanueva, F., Garcia-Lafuente, J., Vargas, J.M., Del Rio, J., Vazquez, A., Real, A., Sanchez, A., 2006. Distribution and circulation of water masses in the Gulf of Cadiz from in situ observations. Deep-Sea Res. 2 (53), 1144–1160.

Csanady, G.T., 1973. Turbulent Diffusion in the Environment. Springer Science, p. 248.

Flather, A., Heaps, N.S., 1975. Tidal computations for Morecambe Bay. Geophys. J. Int. 42, 489–517.

Folkard, A.M., Davies, P.A., Fiuza, A.F.G., Ambar, I., 1997. Remotely sensed sea surface thermal patterns in the Gulf of Cadiz and the Strait of Gibraltar: variability, correlations, and relationships with the surface wind field. J. Geophys. Res. 102 (C3), 5669–5683.

Garcia Lafuente, J.M., 1986. Variability of the Sea Level in the Strait of Gibraltar: Tides and Residual Oscillations. Doctoral Thesis. Spanish Institute of Oceanography, Fuengirola, Malaga, Spain (154 pp).

Garcia-Lafuente, J., Delgado, J., Criado-Aldeanueva, F., Bruno, M., del Rio, J., Vargas, J.M., 2006. Water mass circulation on the continental shelf of the Gulf of Cadiz. Deep-Sea Res. II 53, 1182–1197.

Gomez-Enri, J., Aboitiz, A., Tejedor, B., Villares, P., 2012. Seasonal and interannual variability in the Gulf of Cadiz: validation of gridded altimeter products. Estuar. Coast. Shelf Sci. 96, 114–121.

Gomiz-Pascual, J.J., Bolado-Penagos, M., Vazquez, A., 2016. Soil and water assessment tool. SWAT catchment model to assess Guadalquivir River flow. Sea Technol. 19–21.

González, C.J., Álvarez, O., Reyes, J., Acevedo, A., 2010. Two-dimensional modeling of hydrodynamics and sediment transport in the San Pedro tidal creek (Cadiz Bay): morphodynamical implications. Cienc. Mar. 36 (4), 393–412. https://doi.org/10.7773/cm.v36i4.1624.

Gonzalez, C.J., Izquierdo, A., Alvarez, O., Bruno, M., Mañanes, R., Czerwinski, I.A., Zurita, F.P., 2018. Hazard assessment of bacterial contamination in coastal waters using a metocean modeling system: application to bivalve mollusk harvesting areas in Cadiz Bay (SW Spain). Ocean Coast. Manag. 166, 31–39.

Gonzalez, C.J., Reyes, E., Alvarez, O., Izquierdo, A., Bruno, M., Mañanes, R., 2019. Surface currents and transport processes in the Strait of Gibraltar: implications for modeling and management of pollutant spills. Ocean Coast. Manag. 179, 104869.

Hargreaves, G.H., Allen, R.G., 2003. History and evaluation of Hargreaves equation. J. Irrig. Drain. Eng. ASCE (129), 53–63.

Hargreaves, G.H., Sumani, Z.A., 1985. Reference crop evapotranspiration from temperature. Appl. Eng. Agric. 8, 96–99.

Huertas, E., Navarro, G., Rodríguez-Gálvez, S., Prieto, L., 2005. The influence of phytoplankton biomass on the spatial distribution of carbon dioxide in surface sea water of a coastal area of the Gulf of Cádiz (southwestern Spain). Can. J. Bot. 83, 929–940. https://doi.org/10.1139/b05-082.

Inoue, M., Park, D., Justic, D., Wiseman, W.J., 2008. A high-resolution integrated hydrology–hydrodynamic model of the Barataria Basin system. Environ. Model. Softw. 23 (9), 1122–1132.

Izquierdo, A., Mikolajewicz, U., 2019. The role of tides in the spreading of Mediterranean Outflow waters along the southwestern Iberian margin. Ocean Model 133, 27–43.

Jones, G., 1994. Global warming, sea level change and the impact on estuaries. Mar. Pollut. Bull. 28 (1), 7.

Khoroshevskaya, V.O., 2011. Organic matter content variations in estuaries of Rivers and in the barrier zone of the Taganrog Gulf under the impact of climate changes in the northern catchment of the Sea of Azov. Russ. Meteorol. Hydrol. 37 (6), 397–403.

Le Provost, C., Genco, M.L., Lyard, F., 1995. Modeling and predicting tides over the world ocean. Quantitative Skill Assessment for Coastal Ocean Models. Coast. Estuar. Stud. 47, 175–201.

Matsuzaki, Y., Fujita, I., 2014. Horizontal turbulent diffusion at sea surface for oil transport simulation. Coast. Eng. 1 (34).

Mauritzen, C., Morel, Y., Paillet, J., 2011. On the influence of Mediterranean water on the central waters of the North Atlantic Ocean. Deep-Sea Res. I 48 (2), 347–381.

Mendiguchia, C., Moreno, C., Garcia-Vargas, M., 2007. Evaluation of natural and anthropogenic influences on the Guadalquivir River (Spain) by dissolved heavy metals and nutrients. Chemosphere 69 (10), 1509–1517.

Meng, X.M., Jia, Y.G., Hou, W., Liu, H., Yang, Z.N., 2010. Study on erodibility change of the Yellow River sediment into the sea in the process of consolidation. Proceedings of the ASME 29th International Conference on Ocean, Offshore and Arctic Engineering, Shanghai, China. 1, pp. 757–765.

Narsimlu, B., Gosain, A.K., Chahar, B.R., 2013. Assessment of future climate change impacts on water resources of Upper Sind River Basin, India using SWAT model. Water Resour. Manag. 27, 3647–3662.

Navarro, G., Ruiz, J., 2006. Spatial and temporal variability of phytoplankton in the Gulf of Cadiz through remote sensing images. Deep-Sea Res. II 53, 1241–1260. https://doi.org/10.1016/j.dsr2.2006.04.014.

Navarro, G., Gutierrez, F.J., Diez-Minguito, M., Losada, M.A., Ruiz, J., 2011. Temporal and spatial variability in the Guadalquivir Estuary: a real-time telemetry challenge. Ocean Dyn. https://doi.org/10.1007/s10236-011-0379-6.

Neitsch, S.L., Arnold, J.G., Kiniry, J.R., Williams, J.R., 2011. Soil and Water Assessment Tool. Theoretical Documentation. Version 2009, Grassland, Soil and Water Research Laboratory, Agricultural Research Service, Blackland Research Center, Texas AgriLife Research.

Peliz, A., Fiuza, A.F.G., 1999. Spatial and temporal variability of CZCS-derived phytoplankton pigment concentrations off the Western Iberian Peninsula. Int. J. Remote Sens. 20 (7), 1363–1403.

Peliz, A., Marchesiello, P., Dubert, J., Teles-Machado, A., Marta-Almeida, M., Le Cann, B., 2009. Surface circulation in the Gulf of Cadiz. Part 2: inflow/outflow coupling and the Gulf of Cadiz Slope Current. J. Geophys. Res. 114, C03011. https://doi.org/10.1029/2008JC004771.

Prieto, L., Navarro, G., Rodriquez-Galvez, S., Huertas, I.E., Naranjo, J.M., Ruiz, J., 2009. Oceanographic and meteorological forcing of the pelagic ecosystem on the Gulf of Cadiz shelf (SW Iberian Peninsula). Cont. Shelf Res. 29, 2122–2137.

Proctor, R., Holt, J.T., Allen, J.I., Blackford, J., 2003. Nutrient fluxes and budgets for the North West European Shelf from a three-dimensional model. Sci. Total Environ. 314–316, 769–785.

Reid, R.O., Bodine, B.R., 1968. Numerical model for storm surges in Galveston Bay, National American Society of Civil Engineers. J. Waterw. Harb. Div. 94 (WWI), 33–57.

Relvas, P., Barton, E.D., 2002. Mesoscale patterns in the Cape Sao Vicente (Iberian Peninsula) upwelling region. J. Geophys. Res. 107 (C10), 3164. https://doi.org/10.1029/2000JC000456.

Roe, G.H., Baker, M.B., 2007. Why is climate sensitivity so unpredictable? Science 318 (5850), 629–632.

Ruiz, J., Polo, M.J., Diez-Minguito, M., Navarro, G., Morris, E.P., Huertas, E., Caballero, I., Contreras, E., Losada, M.A., 2014. The Guadalquivir Estuary: A Hot Spot for Environmental and Human Conflicts, Environmental Management and Governance, Volume 8 of the Series Coastal Research Library. pp. 199–232.

Sala, I., Navarro, G., Bolado-Penagos, M., Echeverria, F., Garcia, C., 2018. High-chlorophyll-area assessment based on remote sensing observations: the case study of Cape Trafalgar. Remote Sens. 10 (2), 165.
Sanchez, R.F., Relvas, P., 2003. Spring-summer climatological circulation in the upper layer in the region of Cape St. Vincent, SW Portugal. ICES J. Mar. Sci. 60, 1232–1250.
Sanchez, R.F., Mason, E., Relvas, P., da Silva, A.J., Peliz, A., 2006. On the inshore circulation in the northern Gulf of Cadiz, southern Portuguese shelf. Deep-Sea Res. II 53, 1198–1218.
Simić, Z., Milivojević, N., Prodanović, D., Milivojević, V., Perović, N., 2009. SWAT-based runoff modeling in complex catchment areas – theoretical background and numerical procedures. J. Serbian Soc. Comput. Mech. 3 (1), 38–63.
Soulsby, R., 1997. Dynamics of Marine Sands. Thomas Telford Publications, London (ISBN 0 7277 2584 X).
Stainforth, D.A., Aina, T., Christensen, C., Collins, M., Faull, N., Frame, D.J., Kettleborough, J.A., Knight, S., Martin, A., Murphy, J.M., Piani, C., Sexton, D., Smith, L.A., Spicer, R.A., Thorpe, A.J., Allen, M.R., 2005. Uncertainty in predictions of the climate response to rising levels of greenhouse gases. Nature 433 (7024), 403–406.
Uncles, R.J., 2003. From catchment to coastal zone: examples of the application of models to some long-term problems. Sci. Total Environ. 314–316, 567–588.
van Vliet, M.T.H., Franssen, W.H.P., Yearsley, J.R., Ludwig, F., Haddeland, I., Lettenmaier, D.P., Kabat, P., 2013. Global river discharge and water temperature under climate change. Glob. Environ. Chang. 23 (2), 450–464.
Walter, I.A., Allen, R.G., Elliot, R., Itenfisu, D., Brown, P., Jensen, M.E., Mecham, B., Howell, T.A., Snyder, R., Eching, S., Spofford, T., Hattendorf, M., Martin, D., Cuenca, R.H., Wright, J.L., 2005. The ASCE standardized reference evapotranspiration equation. ASCE EWRI 1–70.
Warner, J., Perlin, N., Skyllingstad, E., 2008a. Using the model coupling toolkit to couple earth system models. Environ. Model. Softw. 23 (10−11), 1240–1249.
Warner, J., Sherwood, C., Signell, R., Harris, C., Arango, H., 2008b. Development of a three-dimensional, regional, coupled wave, current, and sediment-transport model. Predictive Modeling in Sediment Transport and Stratigraphy. 34(10), pp. 1248–1306.
Wilkinson, W.B., Leeks, G.J.L., Morris, A., Walling, D.E., 1997. Rivers and coastal research in the Land Ocean interaction study. Sci. Total Environ. 194–195, 5–14.
Zhang, H., Jiang, Y., Ding, M., Xie, Z., 2017. Level, source identification, and risk analysis of heavy metal in surface sediments from river-lake ecosystems in the Poyang Lake, China. Environ. Sc. Pollut. Res. 24 (27), 21902–21916.